Analytical and Experimental determination of mechanical properties of irradiated materials

by

Deeprodyuti Sen

Roll No. 213me1392

Department of Mechanical Engineering

National Institute of Technology Rourkela

Odisha (India) -769 008

June 2015

Analytical and Experimental determination of mechanical properties of irradiated materials

Thesis Submitted to

National Institute of Technology, Rourkela

for the award of the degree
of

Master of Technology

In Mechanical Engineering with Specialization

"Machine Design and Analysis"
by

Deeprodyuti Sen

Roll No. 213me1392

Under the Supervision of

Prof. Subrata Kumar Panda and Mr. P.V. Durgaprasad

Department of Mechanical Engineering

National Institute of Technology Rourkela

Odisha (India) -769 008

June 2015

NATIONAL INSTITUTE OF TECHNOLOGY

ROURKELA

CERTIFICATE

This is to certify that the work in this thesis entitled "***Analytical and Experimental determination of mechanical properties of irradiated materials using miniature specimen data***" by **Mr. Deeprodyuti Sen** (213ME1392) has been carried out under my supervision in partial fulfilment of the requirements for the degree of **Master of Technology** in Mechanical Engineering with **Machine Design and Analysis** specialization during session 2013 - 2015 in the Department of Mechanical Engineering, National Institute of Technology, Rourkela.

To the best of my knowledge, this work has not been submitted to any other University/Institute for the award of any degree or diploma.

Date:

Prof. ***S*. K. Panda**
(Assistant Professor**)**
Dept. of Mechanical Engineering
National Institute of Technology
Rourkela-769008

SELF DECLARATION

I, Mr Deeprodyuti Sen, Roll No. 213ME1392, student of M. Tech (2013-15), Machine Design and Analysis at Department of Mechanical Engineering, National Institute of Technology Rourkela do hereby declare that I have not adopted any kind of unfair means and carried out the research work reported in this thesis work ethically to the best of my knowledge. If adoption of any kind of unfair means is found in this thesis work at a later stage, then appropriate action can be taken against me including withdrawal of this thesis work.

NIT Rourkela

01 June 2015

Deeprodyuti Sen

ACKNOWLEDGEMENT

I am extremely privileged to be involved in an exhilarating and thought-provoking research project work on "***Analytical and Experimental determination of mechanical properties of irradiated materials using miniature specimen data***". It has enriched my life, giving me an opportunity to work in a new environment of MADAM code and MATLAB. This project helped to expand my understanding.

I would like to express my greatest gratitude to my supervisors **Prof. S. K. Panda**, **P. V. Durgaprasad** and **Dr.B. K. Dutta** for their excellent guidance, valuable suggestions and endless support. I consider myself extremely lucky to be able to work under guidance of such a dynamic personalities and I hope to live up to their expectations.

I would like to express my sincerest gratitude to **Mr. Nevil Martin Jose, Dr. Paramita Mukherjee and Dr. Gayathri N. Banerjee** for guiding me with my experimental activities. I am very much grateful to them for giving their valuable time for me.

I would like to express my sincere thanks to **Vishesh R. Kar, Vijay K. Singh, P.V. Katariya, Sushree Sahoo, Rohan Bhagwat, Snehashis Biswas** (My seniors and batch mate) and all my classmates for their precious suggestions and encouragement to perform the project work.

Finally, I express my sincere gratitude to my parents for their constant encouragement and support at all phases of my life.

Deeprodyuti Sen

ABSTRACT

Determination of bulk properties of in-service irradiated material from micro specimen testing is proposed in the work. Due to complex degradation process of aging experimental reproduction of such aging condition is difficult to obtain. Moreover the availability of such aged material is limited due to high cost. Miniaturized specimens are used for this purpose due to many advantages i.e. they can be directly taken out of in-service materials, ease of irradiating using an external source, less dose to personnel during post irradiation testing etc. So both experimental and numerical method is employed to study the aged material response. For numerical analysis, porous solid Gurson-Tvergaard -Needleman model is used and effect of different parameters of G-T-N model is studied. The G-T-N model is calibrated to fit the Stress-Strain curve of un-irradiated and irradiated curves and Gurson parameters are found. Effects of irradiation on Gurson parameters are studied. These calibrated Gurson parameters are used to simulate a standard CT specimen. Much experimentation is carried out on fabrication and testing of non-standard miniature tensile specimen and results are compared with standard sub-tensile specimens (ASTM-370). Proton irradiation of miniature specimen is carried out at DAE facility VECC with irradiation doses of 0.01, 0.02, 0.04 and 0.06dpa. Same methodology is applied to the irradiated specimen to determine their properties to test the correctness of the proposed methodology.

Contents

LIST OF SYMBOLS

σ_e	von Mises equivalent stress
σ_y	Yield Strength
σ_h	Hydrostatic stress
σ_{ij}	Cauchy stress tensor
$\sigma_{ij}^{/}$	Deviatoric stress tensor
J_2	von Mises yield surface
K,n	Ludwik hardening law parameters
f	void volume fraction
f^*	void volume fraction function
f0/fi	Initial void volume fraction
fc	Critical void volume fraction
ff	Final void volume fraction
q1,q2,q3	Modifying parameters
ƐN	Mean strain for void nucleation
SN	Standard deviation of strain for void nucleation
fN	Void volume fraction at saturated nucleation
f*u/fmax	Modified ultimate void volume fraction

Abbreviations

dpa	displacements per atom
PKA's	Primary Knock-on atoms
EBSD	Electron Back Scatter Diffraction
GTN	Gurson-Tvergaard-Needleman
BR2	Breeder Reactor
RPV	Reactor Pressure vessel
YS	Yield Strength
UTS	Ultimate Tensile Strength
SD	Standard Deviation
COV/CV	Coefficient of Variation
EDM	Electro Discharge Machining
AISI	American Iron and Steel Institute
UEL	Ultimate Elongation
FM	Ferretic/Martensitic
MDBT	Miniature Disk Bend Test
ASTM	American Society for Testing and Materials
LAMMPS	Large Atomic/Molecular Massive Parallel Simulator
CNT	Carbon Nanotube
MD-KMC	Molecular Dynamics-Kinematic Monte Carlo
DMA	Dynamic Mechanical Analyzer
SRIM	Stopping and Range of Ion in Materials
MeV	Mega-electron volts
MADAM	MAterial DAmage Modelling

LIST OF FIGURES

LIST OF TABLES

Chapter 1

INTRODUCTION

1.1 Overview

With the advent of futuristic technologies and machineries, demand for power is increasing every day. In order to cope up with the energy requirement it is necessary to find a powerful, reliable and efficient source. Based on the studies and basic research it has already been proved that the necessity can be achieved by using nuclear power plants. It is not only meet the demand but also come with new challenges for their design, fabrication and their durability. The problems related to nuclear power plant, basically governed by the famous equation given by Albert Einstein "$E=mc^2$"which shows an immense amount of energy can be derived for a small amount of nuclear fuel (uranium, thorium). It is well known that, the amount of energy released in the fission of uranium 235 nucleus is about 60,000,000 times as much as when a carbon atom burns. However, to analyze and controlling of the same is a bigger issue for the research community.

As we know, the nuclear fission occurs due to neutron bombardment and reactor core temperature may reach very high which leads to degradation of material and cause accidental condition. So, it is necessary to find a proper methodology as a first step to predict the life of the in-service material. This is only possible by understanding the complex aging and degradation process as it happens in the real situation during the working. In this regard, many studies have already been taking place through analytical, numerical and/or experimental techniques to understand the degradation processes as well as the material property variation under such extreme condition. It is also true that these all different processes happen in atomic level and to get their desired solution through the said method is not possible every time. Hence, many studies have been carried out to achieve the objective through newly evolved methodology say, multi scale mechanics.

1.2 Multi-Scale Mechanics

In solving a particular problem different approaches may be used based on the system definition and also on which scale it is being defined as per the user. Most of the studies related to graphene sheet and CNT behavior have been analyzed by considering the intermolecular potential for the prediction of the required responses as well as molecular rearrangement in the said material under service condition. The material properties like, Young's modulus, Poisson's ratio etc. can also be obtained using the open ware software LAMMPS. Similarly, in continuum scale the material behavior is being obtained numerically and the corresponding responses are evaluated based on available commercial software and/or homemade computer code. It is observed that all different scale (spatial and temporal scale) of analysis could be done using multi-scale concept. The main objective of multi-scale modeling is to calculate system behavior based on the available information from lower scale. Finally, it aims to suggest some specific recommendation for continuum scale based on the behavior obtained in atomic level. In addition to the above, few specific type of analysis is being used for atomistic level and continuum levels as per the necessity are discussed in the following lines:

- Ab initio models: Solve Schrodinger equations for electrons, electronic degrees of freedom
- Atomistic modeling: Statics, molecular dynamics (MD), kinematic Monte-Carlo (KMC), MD-KMC, atoms are explicitly considered
- Dislocation dynamics: Line defects, dislocation-defect interactions
- Crystal plasticity models: Finite element based poly crystalline (multiple grains) slip systems, dislocation densities, defect densities, texture studies, stress-strain curves, property changes under different ageing mechanisms-creep, fatigue, irradiation etc.
- Micro-mechanical models (continuum damage mechanics) like that of Gurson model help study the fracture.

Based on a Chinese proverb "a picture says thousand words" related to various scale here a pictorial presentation has been shown in Figure 1.1.

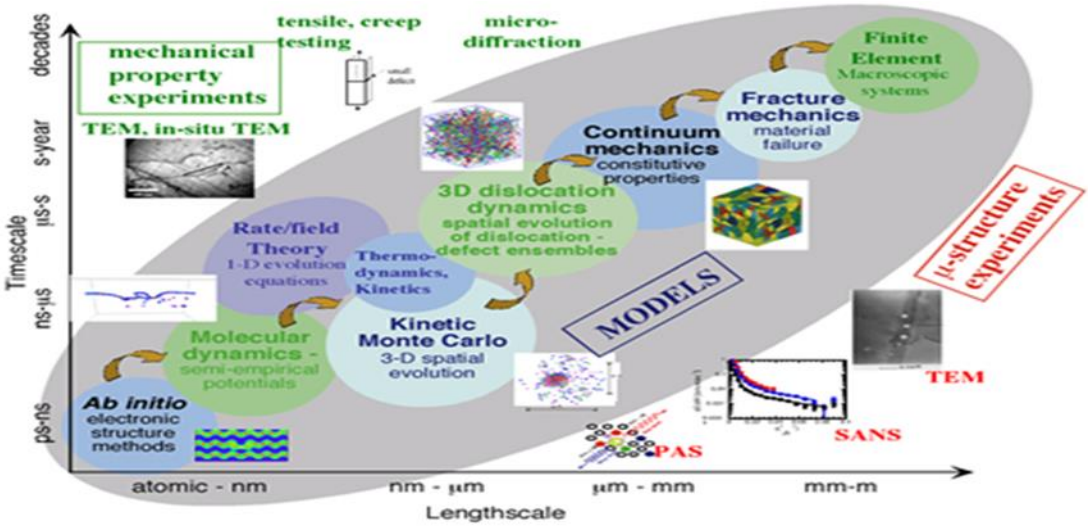

Fig 1.1 Temporal and Spatial domain of different scale used in modelling of system(internet)

1.3 Motivation of the present work

With the advent of futuristic concept of nuclear reactor advances in material is the primary issue. Practical application and realization of such concepts demand high material performance. In advance reactor, materials are subjected to complex degradation process which takes place due to synergic effect of irradiation, temperature, corrosion, and creep. Advancement in materials depends on the understanding of such degradation process under hostile environment, so it is possible to fabricate damage resistant materials. For rapid testing of new materials and alloys it is always desirable to test small volume of material due to high production cost of aged material. Reproduction of complex degradation process of bulk material in laboratories is not only costly but also sometimes not feasible. Irradiation ageing is one of the main damage phenomenon's which an advanced nuclear reactor is subjected to. Neutron irradiation, which most of the reactor materials are subjected to takes a long time to achieve appreciable damage levels for study. To study irradiation aging, ion (proton) beam accelerators are used. The same amount of damage is obtained by ion irradiation faster than what is obtained by neutron irradiation. The advantage of using proton irradiation is that it enables one to study irradiation defect without activation of the specimen in contrary to neutron irradiation. However, the depth

of damage caused by proton irradiation is only about few hundred microns. So, due to the above mentioned constrained in testing small scale testing method is adopted. The main advantage of such testing method is that a very small volume of material is required and small scale specimen can be made from taking small amount of material out of in-service parts which are subjected to complex degradation process. Small scale specimen can also be used to monitor the change in mechanical properties over time for in-service materials. Therefore, the development of micro testing is of great concern. Moreover, linking of mechanical properties obtained from micro testing to the actual bulk properties is a critical task as the small-scale specimen are not standardized i.e. not ASTM standard. So, in the present study both experimental and numerical technique will be employed to study the aged materials.

1.4 Objectives and Scope of the Present Thesis

The present work aims to study irradiation damage in material and develop a methodology in finding out change in mechanical properties like

- Yield Strength
- Ultimate Strength
- Plastic zone parameters i.e. Ludwig's or Holloman's parameters
- Uniform elongation
- Elongation at fracture

All the above properties are found for both miniaturized non-standard and ASTM specimen and a statistical study of amount of deviation is conducted. Proper correlation is found out for properties which show large variation from miniature to ASTM. Irradiation to different dose is carried out on material of reactor interest. An advanced elasto-plastic model i.e. Gurson model is used to numerically simulate stress –strain curve. The parameterized Gurson model is calibrated and effect of irradiation on Gurson parameters are found out. The calibrated Gurson model is then used to simulate a CT specimen and fracture toughness as a function of irradiation is predicted.

1.5 Organization of the Thesis

The general outline of the work presented is given in this section. Chapter 1 is divided into four parts which first consists of a general introduction to the problem at hand. This was followed by the discussion of multi-scale mechanics, which talks about different length and time scale at which problems are dealt with. The following section consists of the motivation of the work which was derived from irradiated material testing in nuclear industries. This was finally followed by the scope of the present work where both experimental and numerical technique is applied to study irradiation damage response. Main objective of numerical simulation was to find out micro-mechanical variable i.e. the gurson parameters for different levels of ageing (irradiation) and use then to simulate standard CT specimen.

Chapter 2 consists of the discussion about basic literatures in the field irradiation study with miniature specimen and application of the advanced elasto-plastic Gurson model.

Chapter 3 is divided in to two parts in which one consists of experimentation with miniature specimens. It consists of basic methodology of experimentation used like sample preparation, testing, results and comparison of results with standards. The other part of the chapter consist of the irradiation programme which has been carried out at VECC for different dpa levels (0.01, 0.02, 0.04, 0.06 dpa).

Chapter 4 discuss about the simulation study which was conducted on irradiated materials using advanced elasto-plastic G-T-N model. Parametric and calibration of gurson parameter for irradiated materials has been shown. A general methodology has been discussed for the use of CT specimen with calibrated Gurson parameters.

Chapter 5 gives an overall conclusion of the present work. It also discusses the significant contributions in this work and the future scope of the research.

Chapter 2

Literature Review

2.1 Introduction

To address the present problem in studying the mechanical behavior of irradiated in-service material, various aspects have to be analyzed to develop a proper methodology. For experimental part of the present work use of miniature specimen for studying different properties and its advantages and disadvantages have been reviewed. For numerical study advanced elasto-plastic Gurson model is implemented to find out the stress strain curve of un-irradiated and irradiated materials.

2.2 Study of irradiation and aging with the aid of Miniature Specimen

Testing of miniature in-service aged material and study of different effects of aging has gained prime importance in industries as micro-specimen can directly be taken out from working component and actual aging condition can be studied. Study of aging is of prime importance to nuclear industries as the synergic effect of creep, temperature, hydrogen embrittlement and irradiation complicate the aging process. Measure of damage due to irradiation and calculation of dpa (displacement per atom) was presented by Olander [1]. Klueh [2] studied comparison of tensile properties of miniaturized sheet and rod specimen with conventional specimen. Experimentation was conducted for SS 316 material for room temperature, 300^0C and 600^0C.Variation in UTS and YS compared to standards were less than 10%(S.D).The study concluded that miniature specimen were suitable for irradiation studies. Panayotou *et al.*[3] conducted studies on design and fabrication of irradiation testing technique. Tensile results were obtained from miniature specimen (AISI SS 316) at high energy irradiation of 14 MeV to a dose level of 10^{18}n/cm^2 or 0.003dpa. Statistically meaningful results were obtained for neutron irradiation. Fabrication technique needs to be refined for accurate ductility measurement. Chen et al.[4] used miniature disk to estimate mechanical tensile properties at an irradiation level of

$1.73*10^{19}$n/cm^2 and temperature 290^o C. The increase in YS and UTS was about 5.5% and 4.2% respectively also a decrease in 12% in UEL was observed. SD for MDBT was less than 3% for strength but very large for variation for UEL. Dai et al.[5] conducted irradiation study of F/M steel in temperature range of 90-370^{0}C to a displacement dose of 3 to 12 dpa. Irradiation hardening was observed to increase till the dose of 10 dpa. Recovery of ductility occurs for 11 and 12 dpa due to high temperature annealing. Rambenberg et al.[6] studied irradiated mechanical properties of AISI SS 304 by miniaturized tensile test method. Shear punch method was used to evaluate strength of irradiated sample which saturated after 5dpa.Ferromagnetic studies were conducted to find austenitic to martensitic transformations. Porollo et al.[7] studied tensile properties and microstructural changes due to irradiation of Fe-Cr alloy with different alloy %(0, 2, 6, 12, and 18%) to irradiation dose of 5.5 to 7.1 dpa. Strength increased w.r.t. dose and ductility decreased. Void swelling due to irradiation was also studied. Olbricht et al.[8] exploited the most fundamental advantage of miniaturized specimen and created prescribed geometry to which allowed small specimen to be directly taken out of the critical components. Creep studies conducted in miniaturized specimen were compared with conventional specimen who revealed size effect in creep behavior. Pahlavanyali et al.[9] conducted thermomechanical fatigue test on miniaturized specimen at temperature range of 100 to 850^{0}C at heating/cooling rate of 5^{0}C/s. Good agreement was obtained between TMF lives of miniature and standard specimen. Miniature specimen showed slightly reduced life. Failure mechanisms for both type of specimen were observed to be same. Digital Image Correlation method was used to measure strain field of micro-specimen by Kartal et al. [10] for the study of local tensile properties of different heat affected zones using micro-specimen and also by Molak et al. [11] for the study of mechanical property of 14MoV67-3 steel after operating time of 0hr to 186000hr at an temperature of 5400C by micro specimen taken out of in- service material. Sharpe et al.[12] studied miniature specimen of A533-B steel of length 3mm and .3 mm square which were made with EDM cutting. Specimens were cut on three different tensile axes to study the effect of anisotropy. The CV for micro-specimen was found about 5% for YS and UTS. The value of yield and ultimate obtained using micro-specimen was 5% less than that of standard conventional specimen. Marini et al.[13] used small notched tensile specimen to study fracture properties of C-Mn steel consisting of large inclusions. Specimens were cut on radial and circumferential direction and test was conducted at 100^{0}C. Experimentation in conjugation with

FE simulation was used to predict toughness. Results obtained indicate critical growth rate criteria makes good estimate of toughness of C-Mn steel. Igata et al.[14] investigated mechanical properties of SS304 and SS316 for various specimen thicknesses (18, 38, 70, 100 & 210 microns) and grain size. Parameters studied were YS, UTS, work hardening exponent (n) and elongation. Elongation observed to decrease with decrease in thickness. Ductile mode of failure was observed irrespective of thickness. Final results indicate the concept of critical value of specimen thickness to grain size ratio as small ratio will show less values of mechanical properties than that of bulk. Rickerby et al.[15] compared miniature specimen properties with bulk as study of neutron damage simulation with help of ion irradiation requires small irradiation area to obtain high displacement rate. Little dependency of YS and UTS was observed but elongation to fracture decreased with decrease in thickness. Negligible influence on thermal creep properties, fatigue crack growth rate and no. of cycles to initiation was observed. For thin flat specimen almost zero remaining ductility was observed after uniform elongation. Byun et al.[16] investigated thickness dependency on miniature specimen of mechanical properties for SA508Cl.3 RPV to find our minimum thickness for bulk like properties and correlation to conventional specimen. Strength dependency was less for specimen thickness above .2 mm. Uniform and total elongation decreased with decrease in thickness as the strain in thickness direction was found to be more than that of the width direction due to plane stress condition dominance. Matijasevic and Almazouzi[17] studied Fe-Cr martensitic steel with different Cr%/wt (0, 2.5, 5, 9, 12.5). Flow properties were determined by tensile test in a temperature range of -160^0C-300^0C. N-irradiation of same material is carried out at 300^0C in BR2 reactor at different dose (0.06dpa, 0.6dpa & 1.5 dpa).

2.3 Application of advanced elasto-plastic Gurson model

Gurson model is to be applied for numerical simulation of tension test of micro specimen and will be experimentally validated. Studied related to Gurson model and aged miniature specimen testing has been reported from time to time. Much literature pertaining to this topic is available but only few important ones are discussed.

Gurson model incorporates the void mechanism during ductile failure. A detailed analysis of growth of isolated void and void interaction effect was reviewed and void growth pertaining to room temperature was reported by Needleman et al. [18].Calculation of R-curve using parametrically tuned G-T damage model was reported by Gabriele [19].The computational results were in good agreement with the experimental results. Only a few parameters of the GTN were tuned (fn,en,sn). Zheng et al. [20] studied effect of different void geometries along plastic deformation and degradation for different forging processes. Pardoen and Hutchinson [21] presented the effect of relative void spacing on coalescence and predicted fracture for a wide range of porosity, initial void shape and stress tri-axiality. Feucht et al. [22] studied damage behavior of high strength and low ductile material using Gurson model extended by Johnson Cook to incorporate shear dominant failures. Hao et al.[23] proposed constitutive relationships during fracture established on the basis of micromechanical cell model. The obtained results showed the methodologies ability to relate between macro and microscopic phenomenon hence capturing physical phenomenon like instability and large deformation during evolution of damage. Tvergaard and Hutchinson [24] identified two mechanism of ductile fracture i.e. void by void and multi-void interaction. Numerical plane strain analysis reviled that for sufficient low initial void fraction void by void mechanism dominates, where as a transition between the two mechanisms is observed at higher initial void fraction affecting the resistance of the material. Li et al.[25] studied effect of mesh size during fracture (ductile) simulation for metals hence connection between fracture strain and mesh size was explored. Logarithmic relationship proposed in eq. 4 of this literature gives insight to trend of mesh size effect seen in FE simulations.

Chapter 3

Experimentation on miniaturized specimen

3.1 Introduction

The materials that make up reactor components are subjected to hostile environment throughout their service life. Many ageing and/or damage phenomenon like temperature creep and irradiation takes place, which degrades the material properties over time. Study of such degradation or ageing proves difficult at times. The major mode of damage of materials in nuclear reactor is mainly damage by irradiation. In this chapter first an understanding of type of damaged caused by irradiation will be discussed and subsequently methodology of using miniaturized specimen for study of irradiation damage will be presented. Finally the irradiation programme carried out for further experimentation.

3.2 Irradiation ageing in materials

Irradiation damage is caused due to interaction of high energy particles like atoms, neutrons, protons and electrons and also gamma rays with material. The material used for rector components are largely steel and alloy which are crystalline in nature. During fission or fusion process, high energy particles are formed and as it strikes the reactor material it displaces the atoms of that material from its lattice points. This is the primary driving force for structural changes caused due to irradiation. Ageing caused by irradiation can be divided in two stages:

- Radiation damage episode: - This event accounts for the interaction of high energy particles with lattice points which causes the atoms to displace. These displaced atoms cause vacancies in the crystal and ultimately come to rest after at interstitial points. Thus a creation of pair of vacancies and interstitial is created know as Frankel pairs. The atoms which are first knocked off by high energy irradiation particle are known as Primary – Knock –Atoms. Once these PKA's are created the travel through the crystal and create higher order knock on. This leads to the creation of displacement cascade within the material. The damage episode is concluded as the PKA's terminate at interstitials. The overall process takes about 10^{-11}s.

- Physical effects of irradiation: - These are subsequent effect to damage events. The effects include growth, segregation, swelling etc.

The mechanical effects of irradiation that manifest after external loading shows increase in YS and UTS but remarkable decrease in ductility and toughness. Experimentation on irradiated materials is a challenge so different approach for experimentation is obtained.

3.3 Need of miniaturized specimen in irradiation study

Irradiation experimentation with standard specimen faces large limitations. The reasons are as follows: -

- Great cost of irradiation.
- Restricted space for experimentation in test reactors
- Fluence gradient in conventional specimen.
- Low depth of damage in ion irradiation (few hundreds of microns)
- Inadequate availability of aged materials.
- Dose to personal during post irradiation testing.

The above are few reasons as to why there is an attempt to miniaturize specimen. One of the distinct advantages of miniaturized specimen is that specimen preparation takes very little volume of aged specimen under study consideration. Hence small volume of material may be directly extracted from in-service material and specimen could be fabricated for testing. The main benefit of this process is that the actual degradation process that occurs in the in-service material can be estimated and more correct prediction of mechanical property can be obtained.

Standardization of specimen is done to decrease the spread in the experimental values of material properties obtained. Role of size effect comes to picture when the dimension of specimen becomes comparable to grain size of the specimen. Hence statistical study of the results obtained from miniaturized test must be conducted and its results must be compared with ASTM standard specimens.

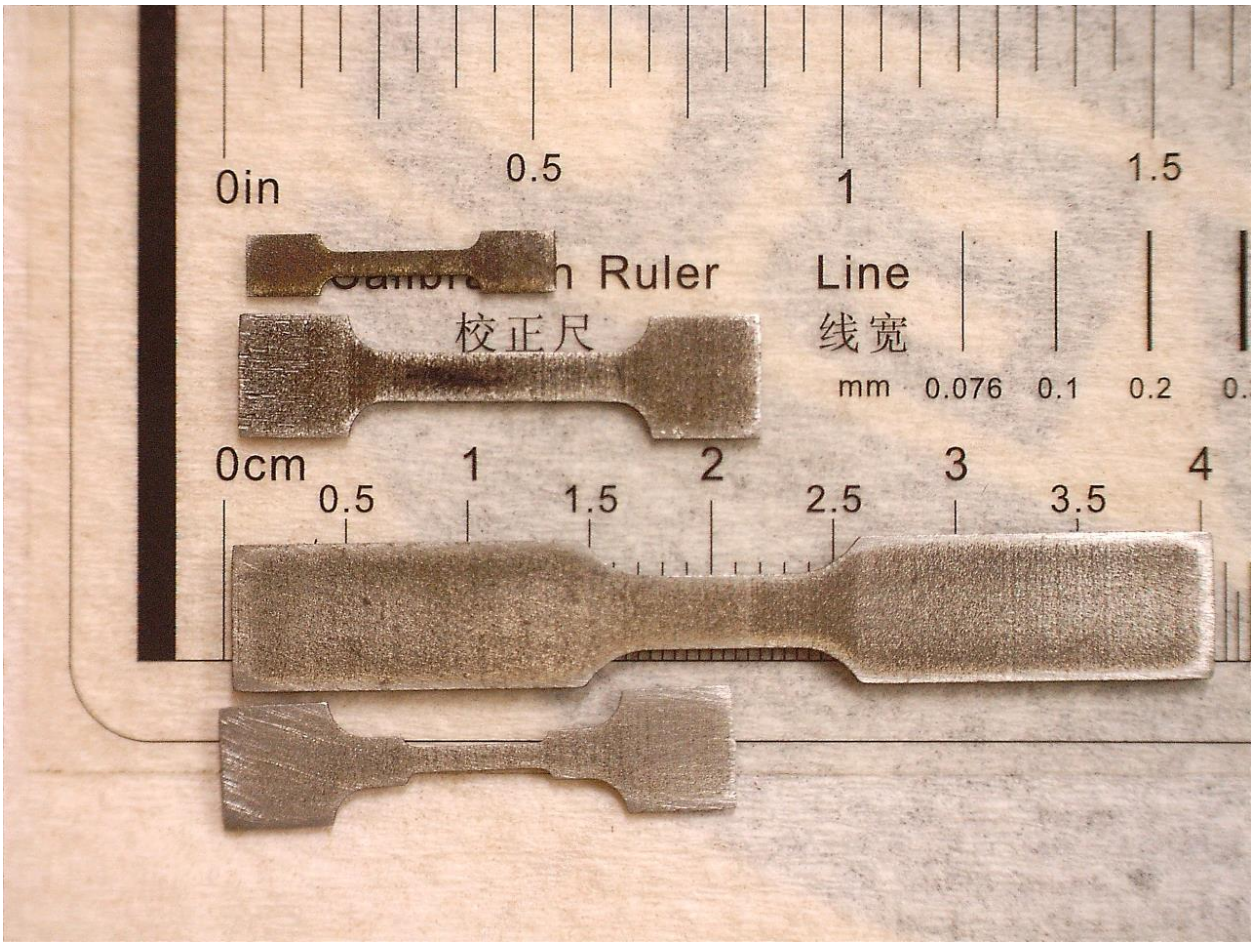

Fig.: 3.1 Size comparisons of miniature and Sub-size tensile specimen

3.4 Experimental Methodology

The first step in experimentation was miniature specimen preparation. As the specimens are non-conventional, no such standards on dimensions of specimens exist. After fabricating the non-standard specimens, polishing of specimen is done to obtain desired surface finish. Although not much variation in mechanical properties was observed with poor surface finish. This may be due to the fact that static tests are not much sensitive to surface finish compared to dynamic tests. After polishing of various types of specimens the one best suited for irradiation programme was sent to DAE felicity VECC for irradiating. The remaining specimens were tested by the help of DMA and the results were compared with ASTM sub-tensile specimen.

3.4.1 Specimen Preparation

Fabrication of non-standard specimen is a complex task. The constraints in the design and dimension are imposed mainly by the experimental machineries used. Also literatures were referred to get a basic idea for specimen dimension. The specimens were cut using EDM wire cutting technique. Constraints that were put up DMA and irradiation facilities are as follows:-

- In irradiation facility at VECC, samples to be irradiated had to glued within the beam area. This constrained suggests the use of flat specimen over round specimen.
- The limit switch of the DMA, which determines the minimum distance between cross-head, is 6.5 mm. Hence any specimen total size will have to be well over 6.5mm.
- Damage profile of proton irradiation is not uniform and the depth of damage depends on the energy of the beam used. Hence the thickness of specimen should depend on the energy of proton beam. SRIM calculation in fig 3.2a, b and c revile the damage profile for three sets of energy i.e. 9MeV, 9.5 MeV and 10MeV. Damage range obtained from SRIM calculation was 222, 243 and 264 microns for energy levels of 9MeV, 9.5 MeV and 10MeV respectively. Hence from this study it was concluded that specimen thickness should be 300($^{+}$_30) microns.

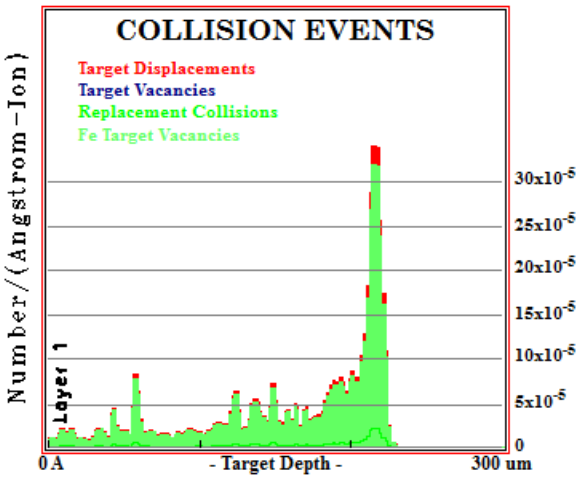

Fig.: 3.2(a) Damage profile for 9MeV proton beam

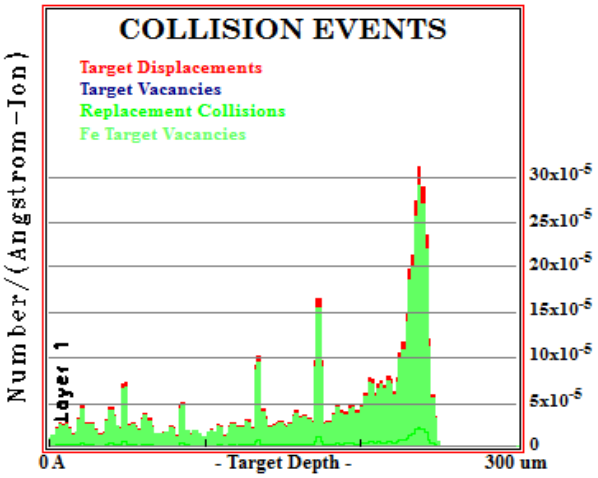

Fig.: 3.2(b) Damage profile for 9.5MeV proton beam

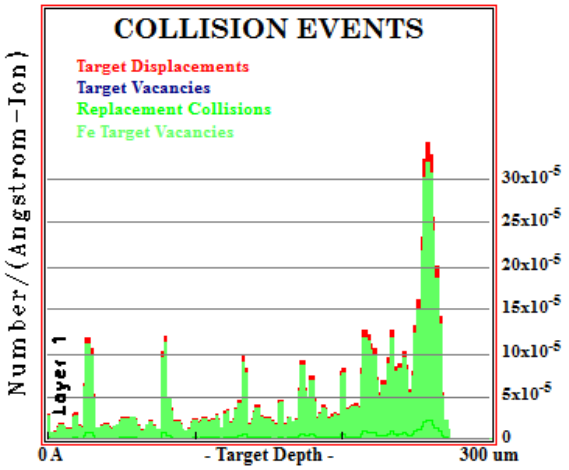

Fig.: 3.2(c) Damage profile for 10MeV proton beam

- The fixtures used in the DMA for flat specimen are friction fixture. So the holding area of the specimen must be high enough to be able to supply the load during test.
- Beam area of irradiation facility considerations should also be accounted so as to have uniform irradiation over the surface.

3.4.2 Types of Specimen

Based on the above constraints three types of specimen were made. The shape and dimension of the specimen are as follows:

1. Single fillet flat (T1 Type): - This type of specimen was initially made without the consideration of irradiation damage. The thickness of the specimen was 500 microns (average). The main purpose of this specimen was to carry out un-irradiated tension test and compare with standards. This specimen also aids in the study of size effect due to thickness variation. The dimension of the specimen is shown in fig 3.2(a).

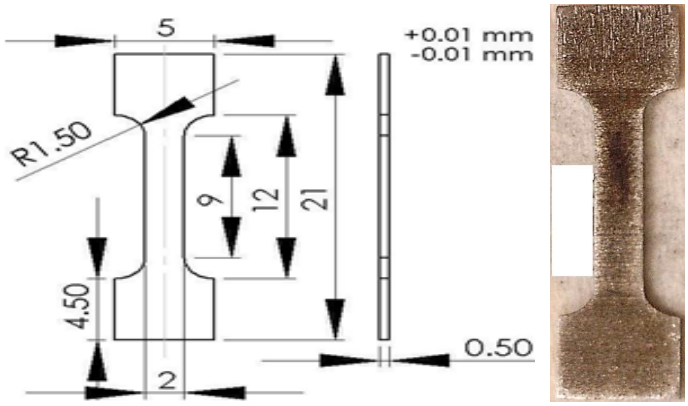

Fig.:3.2(a) Type T1

2. Double fillet flat (T2 Type):- This specimen was fabricated along with T1 type. Due to use of friction type fixture it was anticipates that at higher loads the failure of the material may occur near the holding area. To avoid this problem and force the necking to occur at the central part of the specimen double filleting was done. The thickness and the gauge length were kept the same as T1 type. Details of the dimension are shown in figure 3.2(b).

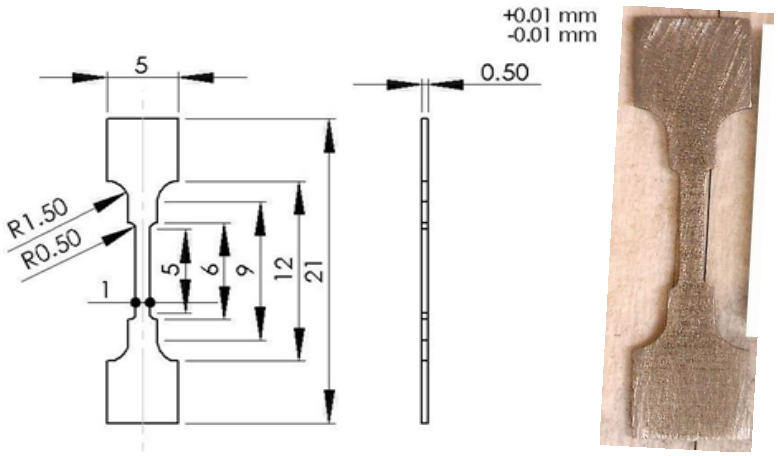

Fig.:3.2(b) Type (T2)

3. Single fillet flat (Type T3):- Type T3 specimen was made satisfying the irradiation aspect discussed in section 3.4.1. The thicknesses of specimens were about 300 microns. This satisfies the criteria for damage depth. Also the total length of the specimen is about 15 mm. This was done by keeping in mind that the uniform beam area is circular with a diameter of 20 mm. The details of the dimension are given in figure 3.2(c).

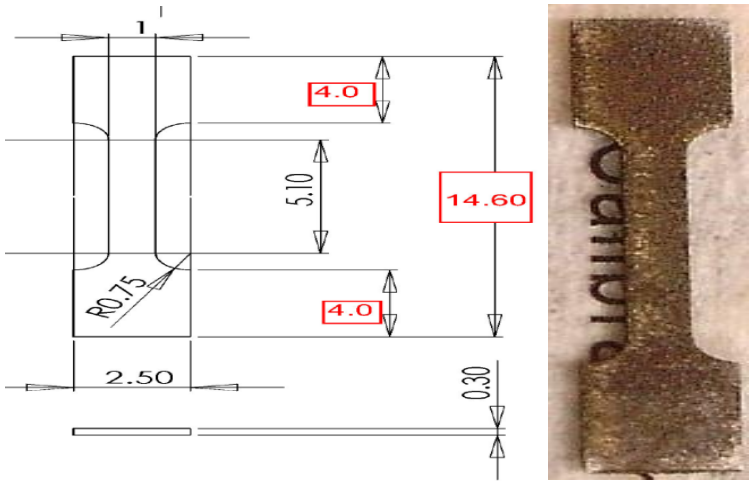

Fig.:3.2(c) Type (T3)

3.4.2.1 Remarks

Trial tests were done on all the three types of specimen. All types of specimen showed necking more or less from the central part. Due to miniature nature of specimen external strain gauge or strain measurement was not possible hence strain was calculated from cross head speed. Cross head speed strain calculation may prove erroneous for type T2 as the gauge area is further away from the clamp portion. Moreover as the necking was observed to occur centrally the type T2 was not considered for further experimentation. Type T2 may be invoked back if some better strain measurement technique is employed in future studies. Hence, it was decided to test on T1 and T3 type specimens. T3 type was the only specimen suitable for irradiation programme so un-irradiated T3 type. There were few testing of T1 type to get an idea of specimen thickness dependency. Finally a comparison of results between miniature specimen and sub-tensile specimen was done.

3.4.3 Testing's on DMA

DMA stand for Dynamic Mechanical Analyzer. Mainly DMA is used to find out complex moduli of polymeric materials. The stimulus and response are out of phase and the phase difference helps in calculation of complex moduli. It is also capable of conducting test conducted by standard Instron machines.

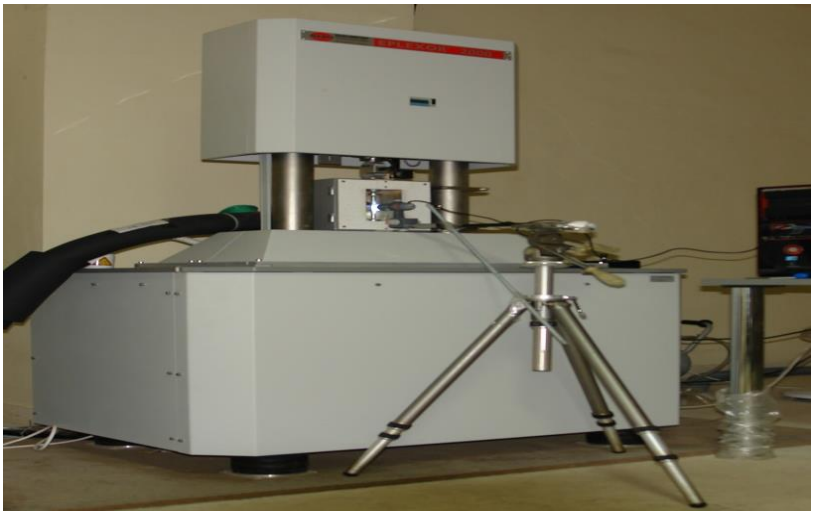

Fig.:3.3 Dynamic Mechanical Analyzer

Basic response study done using DMA:-

- Standard tensile, bending, compression and shear punch test.
- Fatigue test with various types of dynamic loading.
- Determination of complex moduli for polymeric material

Basic specifications of DMA:-

- Load transducers of 500N and 5000N.
- Environmental chamber (-150^0C to 500^0C).
- Various fixtures to carry out different types of tests.
- Large range of strain rate and frequency sweep for dynamic tests

In this study DMA will only be used to conduct tensile test. Tests were performed on T1 and T3 type.

3.4.4 Results and Discussions

A displacement controlled tensile test was performed on T1 and T3 type specimen. Displacement rate of .2mm/min or $3.334*10^{-3}$mm/sec was used. The instantaneous displacement rate is different for different times but the mean was found out to be 0.003346486 for R0055. MATLAB coding for finding out minimum, maximum and mean displacement rate is given in the Appendix. Experimental results of T1 and T3 type specimen for SS304LN material are shown in fig 3.4 and 3.6 respectively.

3.4.4.1 Experimentation on T1-type

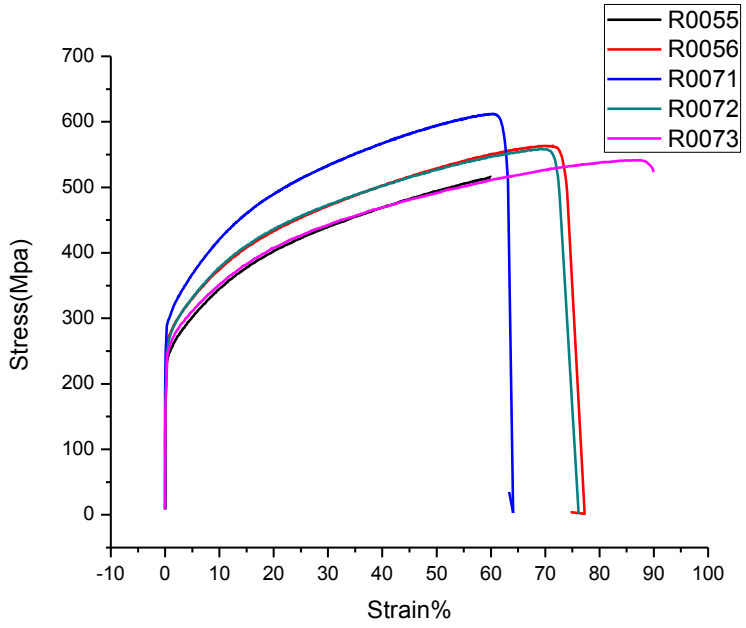

Fig.: 3.4 Engineering Stress Strain curve for T1 type specimen (SS304LN)

T1 type specimen had a thickness of .5 mm. Experiment R0055 stopped before the specimen could reach ultimate point. This was due to the fact that the maximum strain % was given as 60. Comparison of the above mentioned stress strain curves are done on the basis of critical points like YS and UTS. Comparison of stress strain curve cannot be justified by comparing two points as it consists of several points. Hence Ludwik's parameters are found out by fitting the experimental curve. Ludwik's expression is given as:

$$\sigma = \sigma_y + K\varepsilon_p^n \tag{3.1}$$

By using this fitting criteria several points of the stress stair curve can be boiled down to only two parameters. Nonlinear fitting was used in Matlab to find out values of K and n. Sample fitting and residue curve for specimen R0073-T1 is shown below:

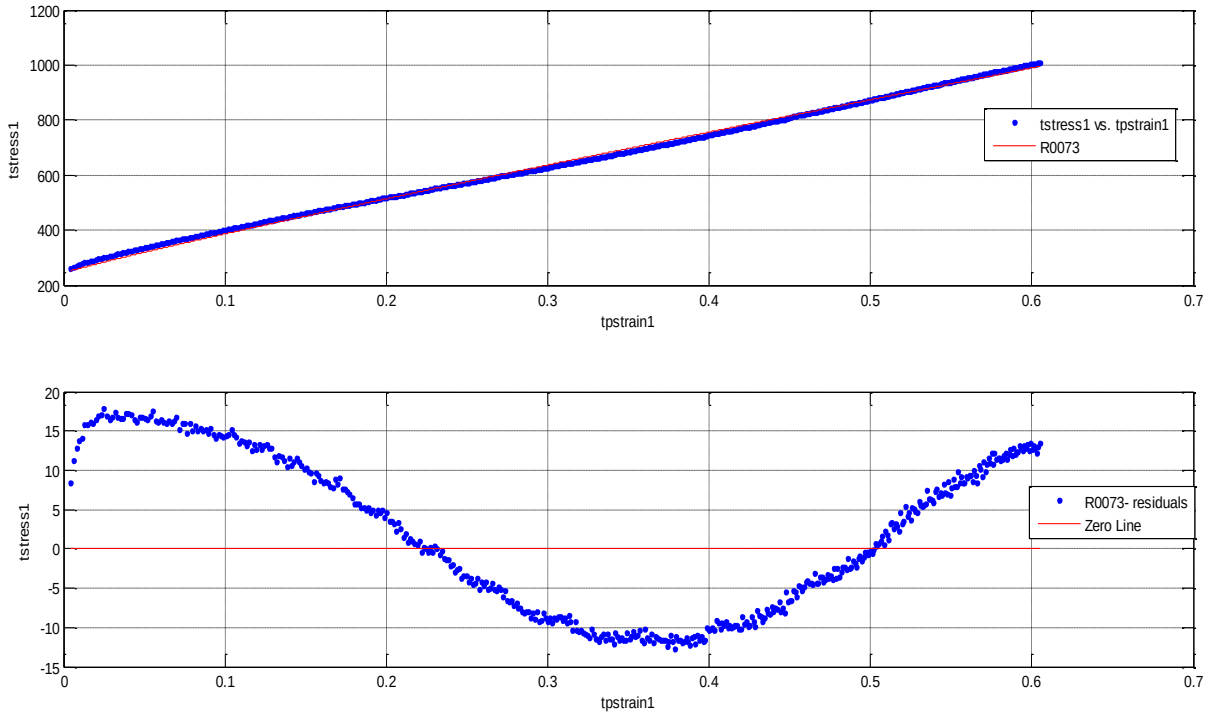

Fig.: 3.5 Fit and residue plot for sample R0071-T1 (R-adj=.9978)

Table representing the values of YS, UTS, K and n for all T1 type specimen are as follows:-

Table 3.1 : Comparison of T1 type specimen

Specimen	Yield Strength(MPa)	Ultimate Strength(MPa)	K(MPa)	N
R0055	232.893 Index no.=6	_	1141	.8742
R0056	253.23 Index no.=5	563.447 Index no.=500	1243	.8926
R0071	288.68 Index no.=7	612.313 Index no.=671	1337	.8633
R0072	246.13 Index no.=4	558.745 Index no.=386	1202	.8466
R0073	244.19 Index no.=4	541.709 Index no.=479	1196	.9251

Similar experimentation was carried out on T3 type specimen. Same methodology as that of T1 type was applied.

3.4.4.2 Experimentation on T3-type

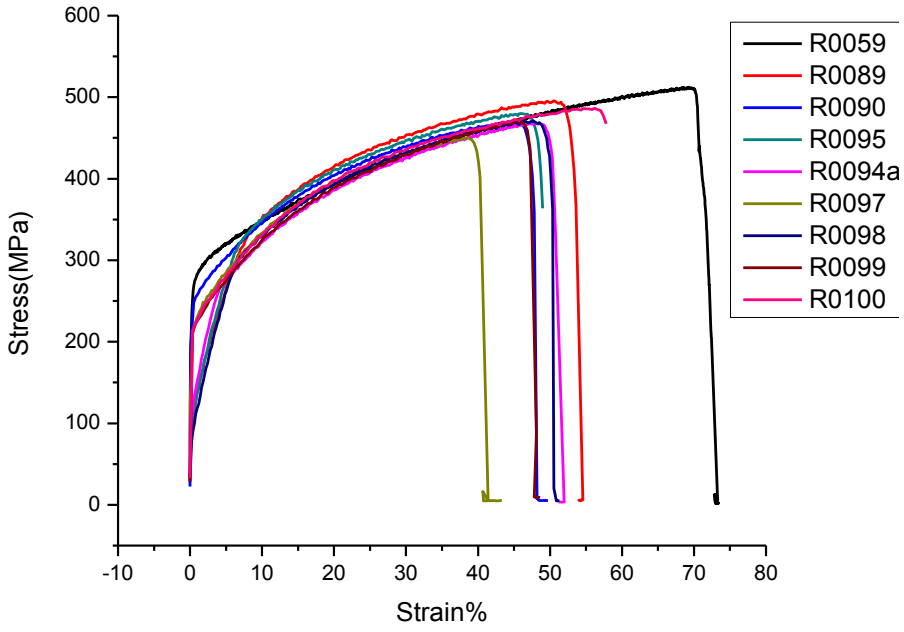

Fig.: 3.6 Engineering Stress Strain curve for T3 type specimen (SS304LN)

Table representing the values of YS, UTS, K and n for all T3 type specimen are as follows:-

Table 3.2 Comparison of T3 type specimen

Specimen	Yield Strength(MPa)	Ultimate Strength(MPa)	K(MPa)	N
R0059	251.336 Index no.=13	512.247 Index no.=1515	1116	.9244
R0089	_	495.497 Index no.=253	1063	.8938
R0090	248.286 Index no.=4	470.724 Index no.=228	1032	.841
R0095	_	479.975 Index no.=231	1018	.747

R0094a	270 Index no.=24	468.831 Index no.=237	1180	.7963
R0097	207.167 Index no.=3	450.256 Index no.=193	1002	.7576
R0098	_	471.278 Index no.=239	1033	.7384
R0099	211.435 Index no.=2	470.663 Index no.=117	1106	.8433
R0100	213.598 Index no.=2	486.483 Index no.=145	1079	.8135

3.4.4.3 Experimentation on T4-type

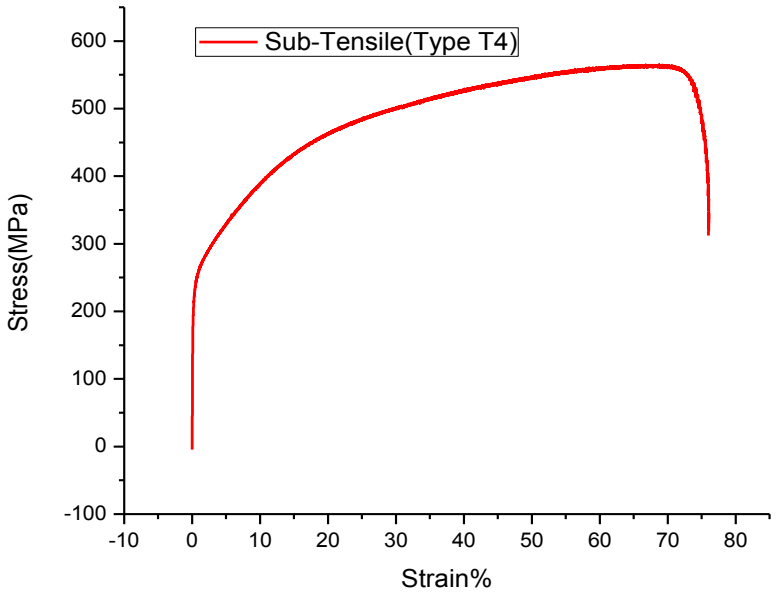

Fig.: 3.7 Engineering Stress Strain curve for T4 type (ASTM 370) specimen (SS304LN)

The details of the dimensions of Sub-tensile T4 type specimen are given in figure 3.8

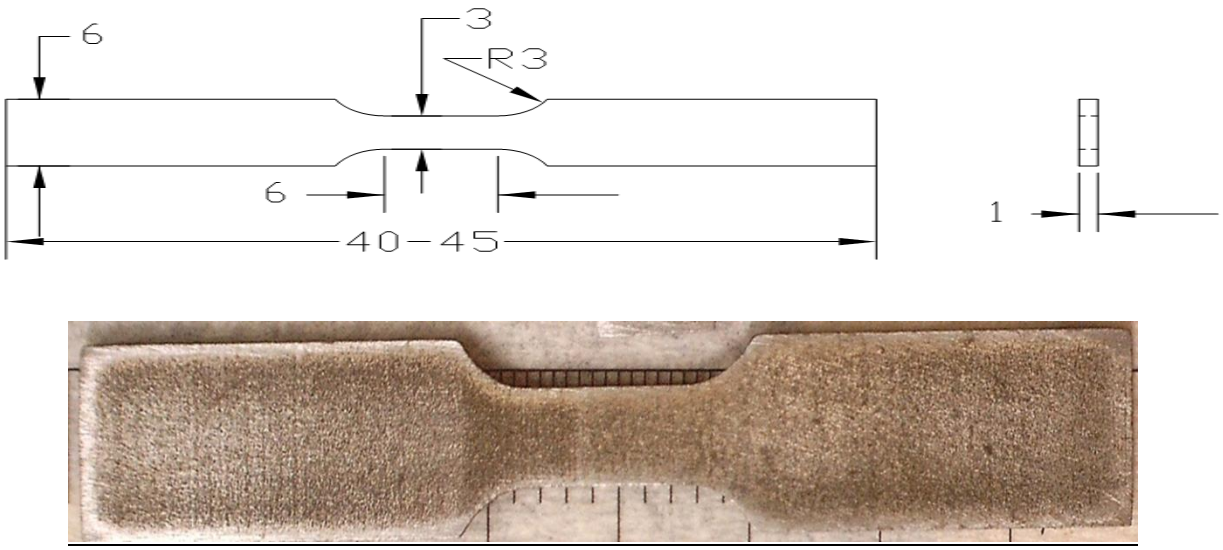

Fig.: 3.8 Dimensions of T4 type specimen (ASTM 370)

Table 3.3 YS, UTS, K and n of T4 type specimen

Yield(MPa)	Ultimate(MPa)	K	N
242.73	564.5461	1190	0.760

3.4.4.4 Data analysis and comparison

Repeatability of experiments on T3 type was found out by statistical analysis:-

Table 3.4 Spread of data obtained from tensile test of T3 type

Statistics	Yield	Ultimate	K	N
Mean	233.61	478.45	1070	.8173
Standard Deviation	23.9935	16.862	53.5006	.0612
C.O.V	.103	.035	.05	.075

The results of the above table show the COV of all the parameters studied is more or less within 10%. Hence repeatability is quit acceptable. As repeatability of experiment is justified, non-

conventional specimen data should yield data comparable to ASTM standards. Some parameters which show appreciable variation is due to the fact that deformation mechanism in miniaturized specimen are different than those of conventional standard specimen. Details of this will be discussed subsequently with literature support. Comparison of parameters stated above for different type of specimen is shown below

Table 3.5 Comparison with A.S.T.M

Specimen Type	Yield(MPa)	Ultimate(MPa)	K	N
A.S.T.M.(T4)	242.73	564.5461	1190	.76
T3 Type	233.61	478.44	1070	.8173

3.4.4.5 Remark and Conclusion

From reference to table 3.5 the percentage error was calculated w.r.t. ASTM standard for T3 type specimen.

- Percentage variation in Yield=3.8% less
- Percentage variation in Ultimate=15.2% less
- Percentage variation in K=10% less
- Percentage variation in n=7.5% more

From the above variation study it is seen that all parameters except Ultimate strength is within acceptable range. From EBSD analysis the mean grain size of the material was found to be 130microns. This indicated that there is less than 3 grains (on an average) in the direction of thickness. Hardening of materials occurs due to obstruction in flow of dislocations around Nano-voids and mainly at grain boundaries. As in the case of T3 specimen very few Grain boundaries are encountered the hardening is less compared to standard specimen (indicated by variation in n). This is one of the major causes for obtaining lower ultimate strength using miniaturized specimen. In Igata et al. [14] a critical ratio of minimum specimen dimension to thickness was stated for SS304 steel which is more than 4. The present specimen (T3) doesn't satisfy this constraint as this requires metallurgical treatment of the material before specimen fabrication.

Two distinct modes of flow instability are observed for a flat specimen where the width is to thickness ratio is large (for T3 specimen it's more than 3). The first mode, diffusion necking, in which necking reduces the width dimension. This is followed by the second mode in which the necking is only restricted along the thickness direction. The second mode forms a band across the width of the specimen inclined w.r.t. the loading/specimen axis. No change in the dimension in width direction occurs in localized necking. Elongation obtained at ultimate is lower than what is obtained from conventional. Byun et al.[16] observed how for miniaturized flat specimen plastic deformation localizes much before plastic instability. Plastic deformation in 2^{nd} mode i.e. in thickness direction is more than that of 1^{st} mode (i.e. width direction). Hence uniform deformation along the thickness is more and reaches criticality (i.e. instability) prior to width. This preferred instability direction accounts for the decreased uniform and total strain. This literature [16] proposed a relationship between corrected total and uniform strain w.r.t. necking angle (localized neck). The correction on the total and uniform elongations obtained from T3 specimen is yet to be done and hence they are not yet reported.

3.5 Irradiation Programme

In the previous section detailed study on miniaturized specimen was done and T3 type was found out to satisfy all constrains. Also comparison of mechanical properties between T3 and T4 (Standard Sub-Tensile) shows acceptable variation. Hence, T3 type specimen was selected for irradiation programme. T3 type tensile specimen for different type of reactor material (SS304LN, FM-T91 and 20MnMoNi55) were made. Type of material doesn't affect the methodology but using different materials help in recheck of the proposed methodology

3.5.1 Irradiation Experiment

Irradiation of the above mentioned materials were carried out at VECC. As mentioned earlier, dpa was used as a unit for measurement of irradiation damage. The unit dpa quantifies the amount of irradiation damage by calculating the ratio of number of atoms which are displaced from lattice site to the total number of atoms in the whole volume. This definition will be made more clear in the consecutive section were dpa calculation for the irradiation programme will be done. Fluence is also a popular unit for expressing neutron irradiation damage but now it is seldom used. This is due to the fact that the dependence of material properties on neutron fluence is dependent on neutron flux spectrum. The example of this phenomenon is shown in the figure (3.9a and b) below:

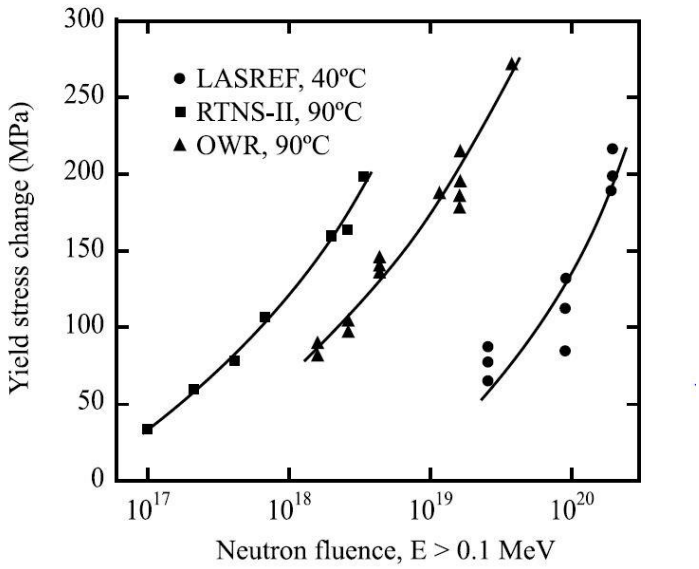

Fig.: 3.9(a) Variation in Yield Strength w.r.t Neutron Fluence for various neutron source[27]

(Courtesy: Fundamentals of Radiation Material Science (G.S.Was Pg11 fig I.1)

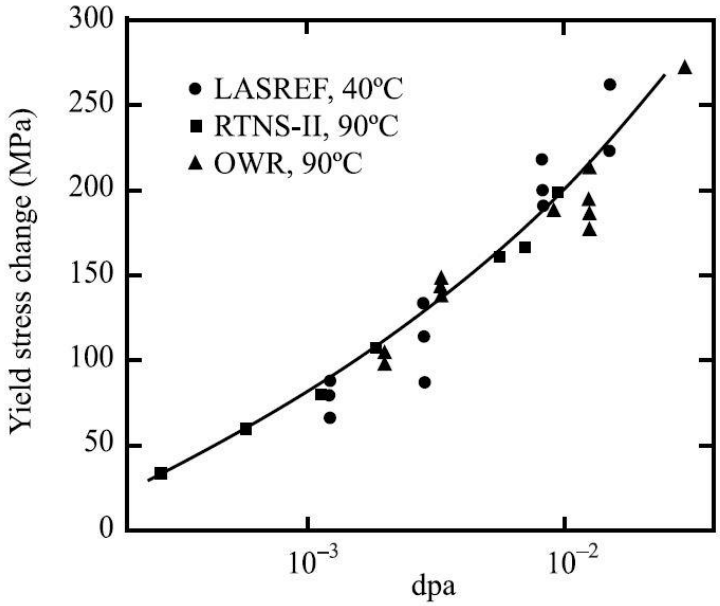

Fig.: 3.9(b) Variation in Yield Strength w.r.t dpa for various neutron source[27]

(Courtesy: Fundamentals of Radiation Material Science (G.S.Was Pg11 fig I.1)

In this study proton irradiation was used. There are certain distinct advantages in using proton irradiation over other source of irradiation. Though the main aim of this study is to evaluate damage due to neutron irradiation but it is problematic to have coherent neutron source. Also such neutron sources are expensive. Hence, better control of dose, dose rate and temperature is possible for ion irradiation. The basic advantages of light ion (proton) irradiation are:

- High dose rate leading to low / moderate irradiation time
- High depth of penetration
- Modest temperature shifts
- Flat damage profile over wide range of depth.
- Less time to reach desired dose limit

3.5.2 Experimental Details and dpa calculation by SRIM

The proton irradiation programme at VECC was conducted at an energy level 9.5MeV. This energy level was decided based on the thickness of the specimen, so that the plate on which the specimen are pasted don't receive any irradiation i.e. all the energy of the proton beam gets dissipated within the thickness. Details of the irradiation conducted are shown in table (3.6 to 3.9):

Table 3.6: 0.01 dpa

Proton energy : 9.5 MeV				**Total 5 specimens**
Date of submission: 11/12/2014				
Date of removal: 12/12/2014				
Starting count = 0				
Final count = 18000				
(1 count = 5 micro coulomb)				
Sl. No.	Material	Specimen type	No.of specimens	dpa
1	FM	T3	2	0.01
2	SS	T3	2	0.01
3	20MnMoNi55	T3	1	0.01

Table 3.7: 0.02 dpa

Proton energy : 9.5 MeV				**Total 3 specimens**
Date of submission: 6/12/2014				
Date of removal: 8/12/2014				
Starting count = 0				
Final count = 37000				
(1 count = 5 micro coulomb)				
Sr. No.	Material	Specimen type	No.of specimens	dpa
1	FM	T3	1	0.02
2	SS	T3	1	0.02
3	20MnMoNi55	T3	1	0.02

Table 3.8: 0.04 dpa

Date of submission: 8/12/2014				**Total 3 specimens**
Date of removal: 11/12/2014				
Starting count = 0				
Final count =				
(1 count = 5 micro coulomb)				
Sr. No.	Material	Specimen type	No.of specimens	dpa
1	FM	T3	1	0.04
2	SS	T3	1	0.04
3	20MnMoNi55	T3	1	0.04

Table 3.9: 0.06 dpa

Date of submission: 6/12/2014				**Total 2 specimens**
Date of removal: 11/12/2014				
Starting count = 0				
Final count = 80000				
(1 count = 5 micro coulomb)				
Sr. No.	Material	Specimen type	No.of specimens	dpa
1	FM	T3	1	0.06
2	SS	T3	1	0.06

In the irradiation programme discussed in the above section shows 4 dpa levels (0.01, 0.02, 0.04 and 0.06 dpa). The dpa level was estimated by the amount of charge that has flow through the specimen area. S.R.I.M. calculation yields the total no. of vacancies that are created due each ion collision. Sample calculation for 0.02 dpa :

1 proton= $1.6*10^{-19}$ C; 1C = $6.25*10^{18}$ protons;

1count= 5μC; (VECC specifications)

1 count= $3.125*10^{13}$protons;

37000 count= $1.15625*10^{18}$protons (from table 3.7)

Beam area was circular with a cross-section of 20mm. Hence, beam area= π cm^2.

Fluence= $3.68046*10^{17}$ protons/cm^2;

Exposed area of the specimen (T3) = (14.6*2.5)-(5.1*1.5)-(π*(.75)^2) =27.083mm^2 =0.27083 cm^2

Total volume of specimen (T3) = 8.124mm^3= $8.124*10^{-3}cm^3$

Although SS304LN is an alloy, its major constituent is iron. Hence, the calculation for total no. of atoms in the specimen is based on the assumption that the specimen consists of only iron atoms. So,56 gms of iron consists of N_A no. of atoms. So 1gms consists of N_A/56 no. of atoms.

ρ_{iron}= 7.87 gm/cm^3 ; m_{iron} = $7.87*8.124*10^{-3}$ = 0.0639 gms;

No. of atoms= (N_A/56)*0.0639 = $6.871*10^{20}$;

Now,

$$dpa = \frac{Fluence * Area\_of\_specimen * (vacancies / ion)}{Total\_atoms} \quad (3.2)$$

No. of vacancies per ions are calculate by SRIM software for 9.5 MeV to be 113.

Putting all the above calculated values in eq(3.2) we get calculated dpa to be 0.016 dpa.

Chapter 4

Simulation Study

4.1 Introduction

The last chapter detail analyses of experiments on un-irradiated samples were conducted. As indicated earlier the coulomb barrier iron based alloy was about 7 MeV. Hence, the irradiation process has led to activation of the sample. So testing on the irradiated samples can be conducted only after radiation level is below permissible range. Meanwhile, to develop a simulation methodology to obtain Gurson parameters for irradiated specimen, experimental results for irradiated specimen was taken from literature [17]. Gurson parameters for irradiated specimen were derived with a higher objective in mind. Gurson parameters depict the manner of void nucleation, growth and coalescence when the material is subjected to external load or displacement fields. These void parameters dictate the mechanism of ductile fracture. Hence, the Gurson parameters that would be derived by calibrating stress strain curve for tensile specimen can serve as input for simulation of standard fracture specimen (CT), to evaluate fracture toughness. Direct testing of irradiated CT specimen is a costly affair and for higher dpa levels it might be not feasible. Hence, this chapter attempts to find an alternative method.

4.2 Mechanics of porous solids and Damage mechanics

In defect free materials (ideal) fracture initiates after flow instability. This occurs due to the fact when strain hardening cannot keep pace with reduction in area. Ideally a pure material should have 100% area reduction before failure. However this is not the actual case. This is due to the presence microscopic voids and flaws present in the material and also due to nucleation of new voids as the material is under straining. So for real materials softening occurs due to both geometric reasons (reduction in area) and void mechanisms. Hence, a pure elasto-plastic analysis doesn't reflect full physical reality of deformation especially after tensile flow instability. Figures 4.1 and 4.2 depict the above fact pictorially.

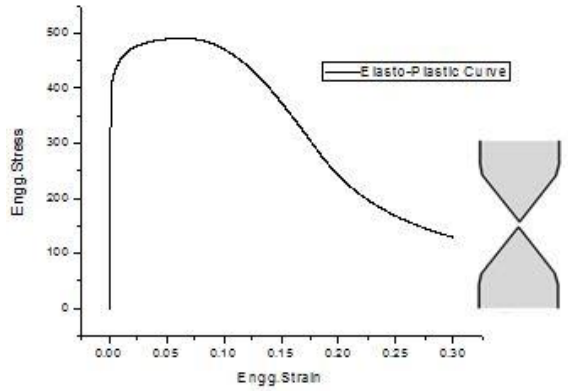

Fig.: 4.1(a) Elasto-Plastic analysis

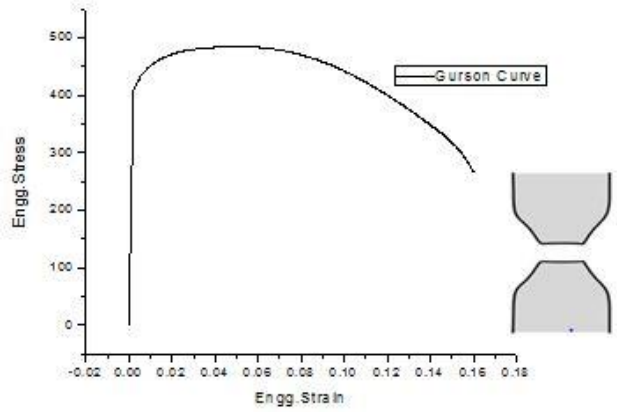

Fig.: 4.1(b) Gurson analysis

It is seen that (from fig 4.1(a)) the curve asymptotically reaches zero stress. Hence prediction of total elongation is not possible via this analysis. From the figure 4.1(b) it seen that Gurson analysis gives more realistic stress strain curve as void mechanism leads to final fracture prediction.

Two different type of void growth model:

- Uncoupled Void-Growth Model: - Uncoupled model also known as explicit model in which the main aim is to determine the dependence of void growth rate on imposed stress strain fields. In explicit model the stress strain field is known over the domain by

analytical or experimental method, and then an explicit equation relating void growth rate and imposed stress strain field is used to find the final void size. Failure of the material is justified by defining a critical void volume, if final void volume fraction is more than critical material is said to fail.

- Coupled Void Growth Model (Gurson Model):- The coupled or the implicit model contains the micro-mechanism of void in the constitutive equations itself. The Gurson model is a modified flow rule in which void volume fraction (f) is taken as a parameter. When f=0 then the Gurson flow rule becomes identical to J2 flow rule. Gurson flow potential is expressed as:

$$\varphi = \frac{\sigma_e^2}{\sigma_y^2} + 2f\cosh\left(\frac{3\sigma_h}{2\sigma_y}\right) - 1 - (f)^2 = 0 \quad (4.1[18])$$

Where $\sigma_e = \sqrt{\frac{3\sigma_{ij}^{'}\sigma_{ij}^{'}}{2}}$, $\sigma_{ij}^{'} = \sigma_{ij} - \frac{1}{3}\delta_j^i\sigma_{kk}$, $\sigma_h = \frac{1}{3}\delta_j^i\sigma_{kk}$

(σ_e =von Mises equivalent stress, σ_{ij} =Cauchy Stress tensor, $\sigma_{ij}^{'}$ =Deviatoric Stress tensor, σ_h =Hydrostatic Stress tensor & σ_y =Yield Strength)

Eq(4.1) gives the yield potential which shows an exponential dependence on stress tri-axality which is defined as the ratio of hydrostatic stress to yield strength. In defect free (ideal) solid change is volume is negligible in plastic deformation but due to growth of void in the solid plastic flow becomes dilatational. This is why there is rapid loss load carrying capacity and a highly non-linear softening nature is observed. Fig 4.2 & 4.3 show the plot of Gurson and J2 yield function in principal stress space respectively. Figure 4.2 shows closing of yield surface as hydrostatic component of stress increases hence incorporating the dependence of void growth rate on hydrostatic stress.

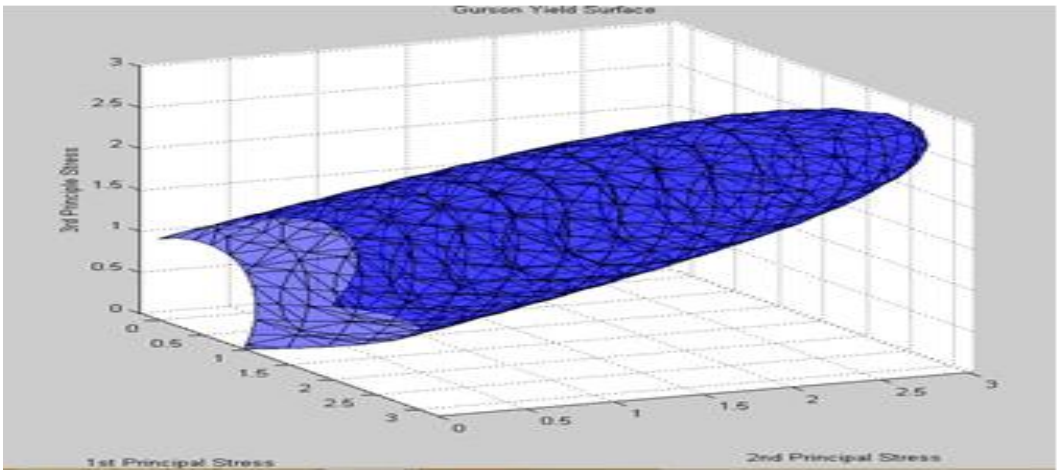

Fig. 4.2 Gurson Yield Surface

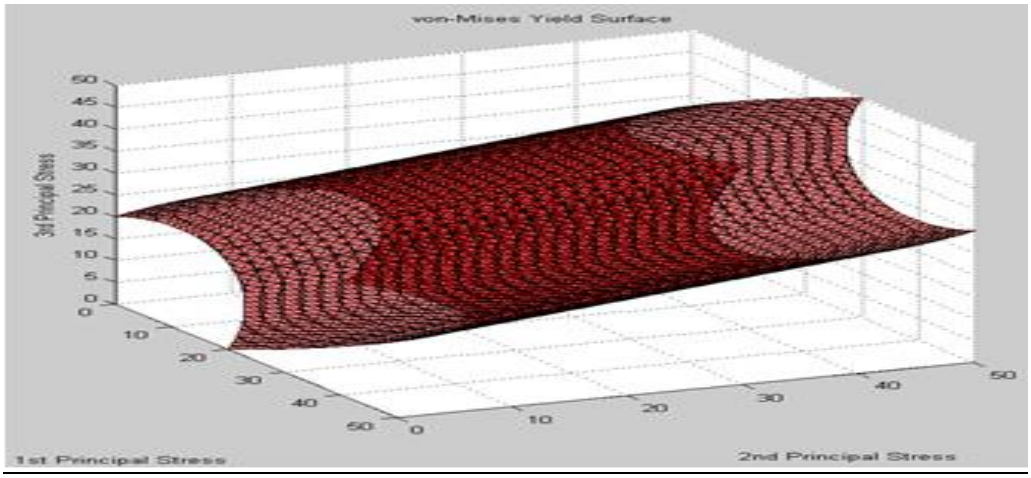

Fig.4.3: J_2 Yield Surface

4.3 Modified Gurson Model (G-T-N)

During failure of ductile material smooth varying deformation pattern grows into a highly restricted deformation. This is the concept of necking. Void interaction takes place during localization through coalescence. To account for the void interaction effect, adapting constants (q1=1&q2=1.5) were introduced by Tvergaard for the yield relation.

With the onset of coalescence there is a prompt loss in load carrying capacity takes place with little change in the void volume fraction. To incorporate this effect in the yield model the void fraction (f) is replaced with a void fraction function (f*). Including all the above mentioned

effects the modified Gurson model was put down by the combined work of Gurson, Tevergaard and Needleman as:

$$\varphi = \frac{\sigma_e^2}{\sigma_y^2} + 2q_1 f^* \cosh(\frac{3q_2\sigma_h}{2\sigma_y}) - 1 - (q_1 f^*)^2 = 0 \quad (4.2[18])$$

Where

$$f^*(f) = f \qquad (f \le f_c)$$

$$f^*(f) = f_c + K(f - f_c) \qquad (f \ge f_c)$$

The variation of void function (f*) is shown pictorially in Fig.4.4. It can be seen from this figure there is a sudden rise in the slop of the function f* after f=fc=.02. This is the critical value of f at which void coalescence starts. K is sometimes referred as the 'accelerating factor' which signifies the rapid increase in the function f* due to coalescence. The value of K is basically the increased slope of the void volume fraction function given by:

$$K = \frac{f_u^* - f_c}{f_f - f_c} \qquad (4.3[18])$$

At f=ff=.1817 the f* becomes constant and this signifies the complete loss in load carrying capacity of the material i.e. f*(ff) =fu*=1/q1.

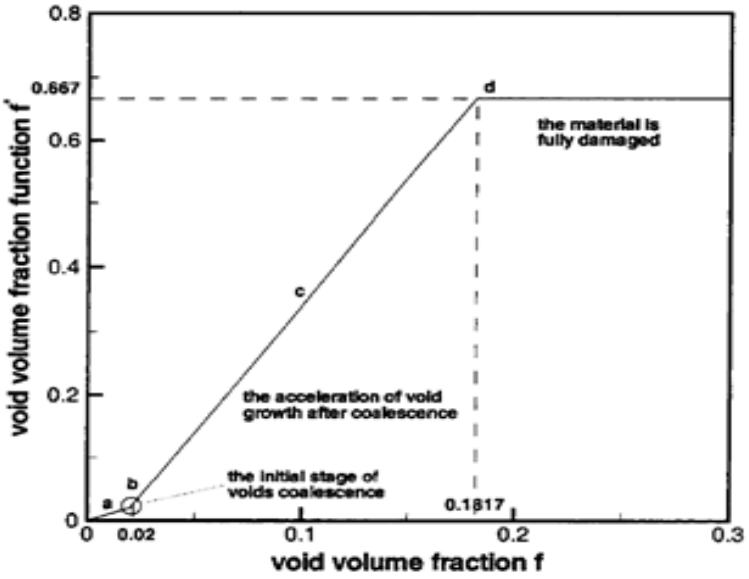

Fig.4.4: Void Volume Fraction Function (f^*) [26]

4.4 Simulation Methodology

A displacement control tensile test was simulated in MADAM (MAterial DAmage Modeling is a finite element program developed and maintained by computational mechanics section, Reactor Safety Division, BARC) code. General inputs required for an Elasto-Plastic finite element analysis is the yield criteria, hardening law and the flow rule. The hardening law is derived from uniaxial tests stored in numeric form. The general procedure which is followed for generating results in the discussed in preceding section is defined as:

- Convert obtained engineering stress-strain data from literature to true-plastic strain and true stress.
- Extrapolate the above converted data beyond ultimate point using Ludwik's or Holloman's strengthening law. The generated true stress & true plastic strain data is a matrix level stress strain data with no defects due to both geometry and material impurities like voids and flaws.
- Parametric study is conducted to comprehend how different Gurson parameters affect the stress strain curve. Only certain parameters were studied in the parametric study (f_o, f_n, f_c and f_f) as they are the dominant parameters which change with material while others are parameters are material invariant.
- From the knowledge of parametric study calibration of Gurson parameters is done by fitting literature data for different dpa levels.

4.5 Results and Discussions

The G-T-N Model is a parameterized flow rule. For applying it to different metals calibration of different parameters are required. The Gurson parameters required for micromechanical analysis are shown in the following table:

Table: 4.1 Gurson Parameters

Name of the parameters	Symbol
Initial void volume fraction	f_0/f_i
Critical void volume fraction	f_c
Final void volume fraction	f_f
Modifying parameters	q_1
	q_2
	q_3
Mean strain for void nucleation	ε_N
Standard deviation of strain for void nucleation	S_N
Void volume fraction at saturated nucleation	f_N
Modified ultimate void volume fraction	f^*_u/f_{max}

Each parameter sensitivity is investigated by varying significant parameters (like f_i,f_n,f_c,f_f) independently one at a time while keeping others fixed.

Displacement control tensile test simulation is carried out. The engineering stress-strain curve is obtained for each run. The number of variations carried out for a particular parameter may vary from one to another. From the help of this parametric study a general understanding of the various gurson parameters are obtained, which later on is used to fit experimental Stress-Strain curve which helps in calibrating the Gurson parameters for a particular metal/alloy.

4.5.1 Parametric Study

1. Initial void volume fraction (f_i/f_0)

   The engineering stress strain curves for different values of f_i are:

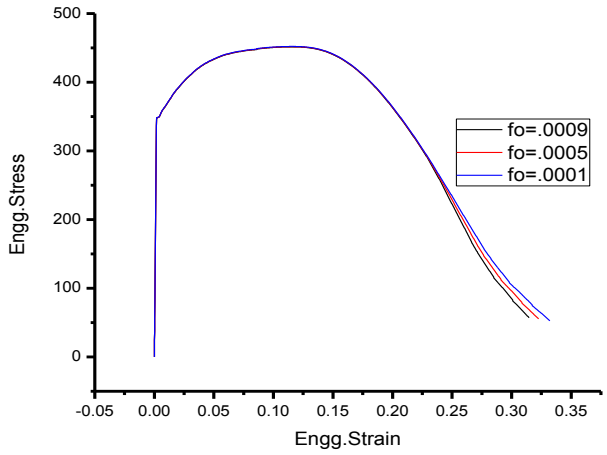

Fig.4.5(a): Initial void fraction (f_i)

The initial void volume fraction (fi) is related to the inclusions and the so called primary voids. They are inherent flaws which are created during manufacturing of the material. This parameter is primarily estimated from the micrography of the material and calibrated by analyzing test specimens. As seen from fig.4.5 (a) the effect of variation of fi is very negligible during initial plastic deformation and gets prominent only neat the failure zone. This is because the initial void volume fraction increases the probability of void nucleation affecting the later part of the plastic zone. Larger initial void volume will produce larger void fraction under loading and as the volume fraction equals the critical void volume, void coalescence occurs.

2. Variation of fn

   The engineering stress strain curves for different values of fn are:

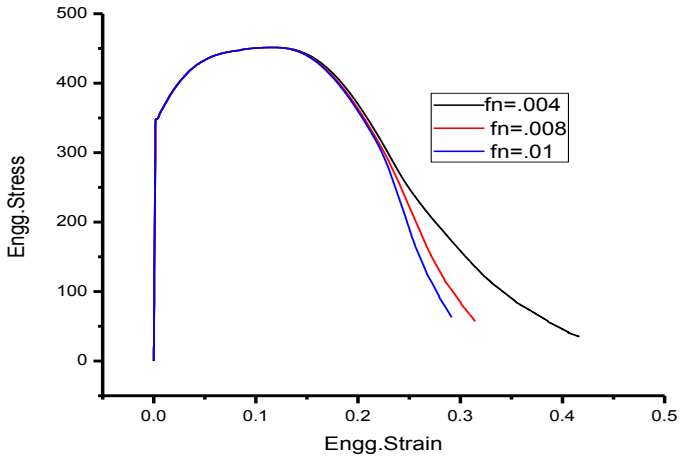

Fig.4.5 (b): Nucleating void volume fraction (fn)

To account for the nucleation phenomenon and accommodate it in the Gurson model, total growth rate of porosity is the summation of growth rate of preexistent voids and rate of new nucleating void. Nucleating rate depends on both stress and strain. In this study however strain controlled nucleation is used because of simplicity. In strain dictated model, nucleation rate is directly dependent on fn. Hence, more nucleation rate, steeper is the softening.

3. Critical void volume fraction (fc)

   The engineering stress strain curves for different values of fc are:

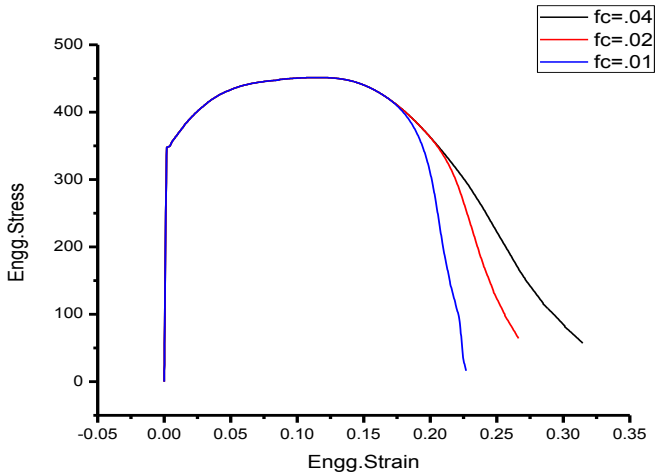

Fig.4.5 (c): Critical void volume fraction (fc)

From fig.4.5 (c) it is seen that variation in critical void fraction causes much appreciable change in the nature of the stress strain curve. This is because the value of fc dictates the void fraction at which coalescence of void start. Coalescence is due to internal necking between two adjacent void which leads to rapid loss of strength. Thus lower the value of fc steeper the slope of the softening part of the stress strain diagram. The rapid drop in stress can also be explained with the help of fig.4.4 which shows the rapid increase in the slope of the void volume fraction function denoted by K in eq. [4.3].

4. Final void volume fraction (ff)

   The engineering stress strain curves for different values of ff are:

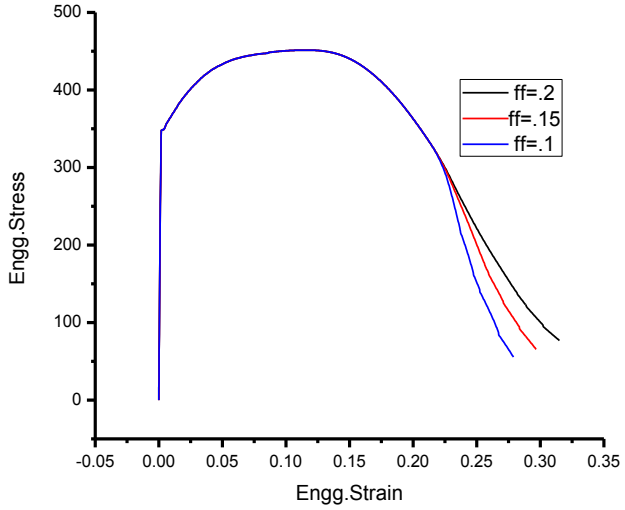

Fig.4.5 (d): Final void volume fraction (ff)

Final void fraction is the void fraction at which complete loss in load carrying capacity takes place. Lower the value of this fraction faster the curve falls to final fracture. When the value of the void volume fraction reaches ff the void volume fraction function becomes fmax. fmax is the largest value of the void fraction function shown in fig. 4.4. From the fig. 4.5 (d) it is seen that this parameter affects the part of the curve very near to fracture point. Hence, this parameter is useful for calibrating the final drop observed during fracture.The modifying parameters q1, q2andq3 are generally not changed. The standard deviation of stress for nucleation (Sn) and the

modified ultimate void volume fraction (fmax) has not much effect on the material behavior and thus these parameters are also kept unchanged.

4.5.2 Calibration of Gurson parameters

Fe-Cr steel was conducted by Matijasevic and Almazouzi at dose level of 0, 0.06, 0.6 and 1.5 d.p.a. The Engineering Stress Strain curve obtained from the literature is shown below:

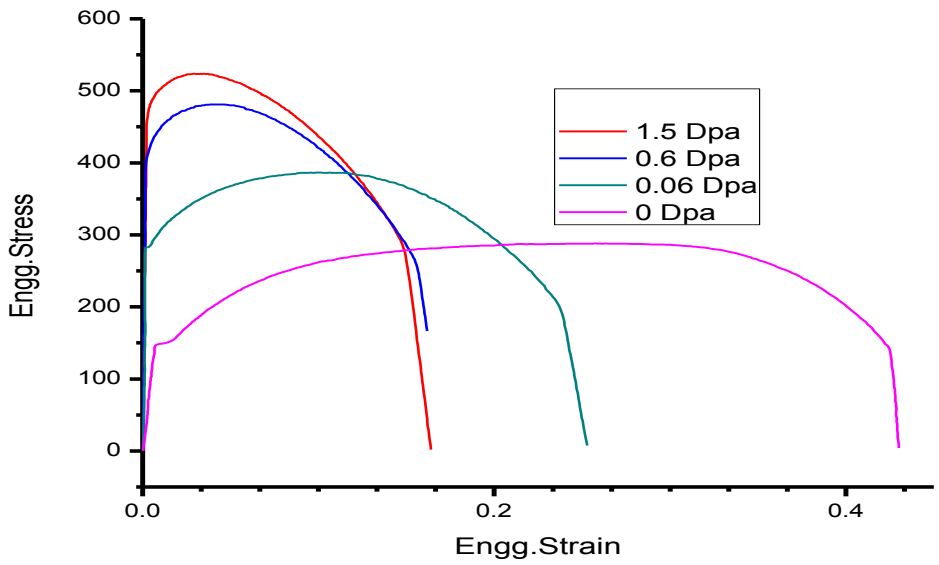

Fig.4.6: Unirradiated and irradiated stress-strain curve[17]

With reference to the previous parametric studies calibrations of the parameters are made.

- 0 dpa (un-irradiated)

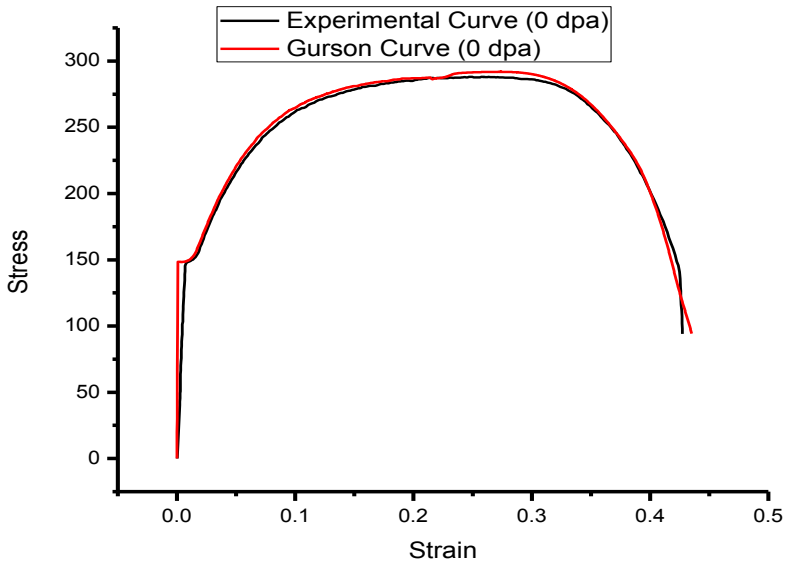

Fig.4.7(a): 0-dpa calibration

- 0.06 dpa(Irradiated)

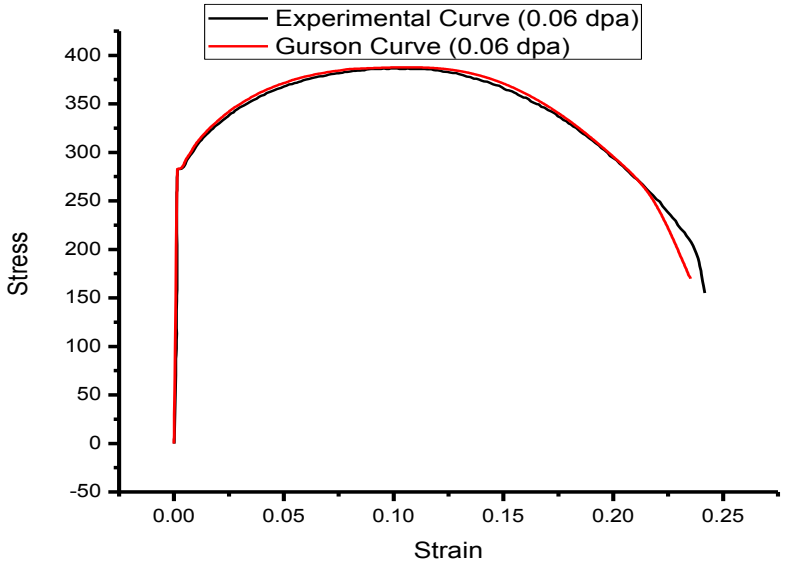

Fig.4.7(b): 0.06-dpa calibration

- 0.6-dpa (Irradiated)

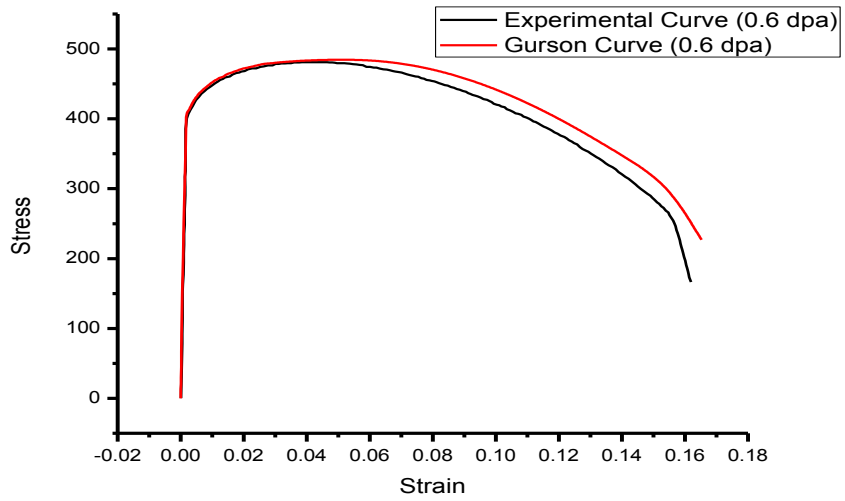

Fig.4.7 (c):0.6-dpa calibration

- 1.5-dpa (irradiated)

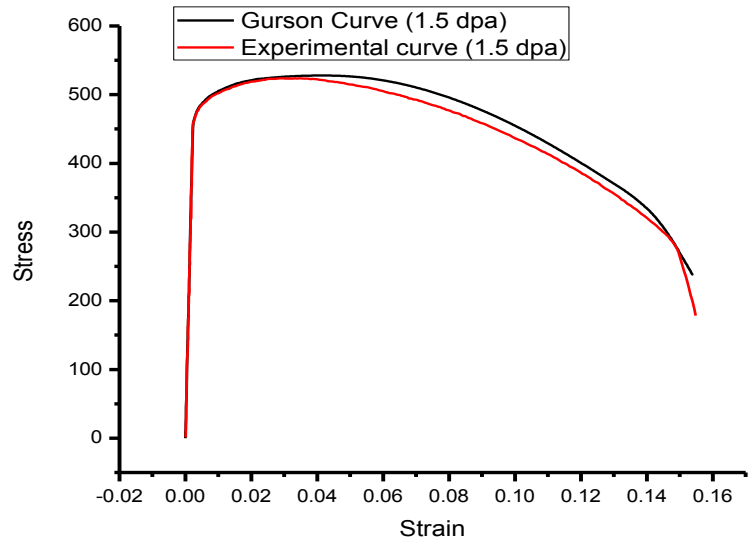

Fig.4.7 (d): 1.5-dpa calibration

It is interesting to note that during calibration same Gurson parameters were used for both irradiated and un-irradiated specimen. The calibrated parameters are show in Table 4.2.

Table : 4.2 Calibrated Gurson Parameters

Name of the parameters	Symbol
Initial void volume fraction	f_0/f_i=5e-4
Critical void volume fraction	f_c=0.015
Final void volume fraction	f_f=0.1
Modifying parameters	q_1=1.5, q_2=1, q_3=2.25
Mean strain for void nucleation	ε_N=.3
Standard deviation of strain for void nucleation	S_N=.1
Void volume fraction at saturated nucleation	f_N=0.004
Modified ultimate void volume fraction	f^*_u/f_{max}=.63

4.5.3 Proposed methodology for toughness evaluation computationally:

Growing crack analysis simulation computationally is a tricky job as it includes re-meshing to accommodate crack growth which becomes cumbersome for elastic-plastic problems**.** But on the contrary use of the parameterized G-T-N model gives the simulators a distinct advantage as the failure criterion of an element is inbuilt. As the elements defined in the crack front are strained the value of the void fraction function increases and reaches the ultimate void fraction which indicates that element's gauss point's total loss in load carrying capacity, henceforth signifying the growth of crack through a distance of half of the element size. Physically the growth rate of crack depends on length scale of material like intra void distances, inclusion spacing etc. So for FE simulation to give correct prediction, element size should be tuned. For this reason the mesh size in the crack plane is refined to .2 mm (inclusion spacing). The detailed procedure to generate J-R curve via simulation are as follows:-

- Standard CT specimen is simulated.

- Mesh along the crack front is made uniform and of size .2mm^2.
- Tuned G-T-N model (from the above tensile test) is used as material properties for various dpa levels.
- Pin Load vs pin displacement is found out.
- Crack growth vs pin displacement is found out from information about void fraction for gauss point of each element.
- ASTM designation E 1820-13 is used to post process the obtained result from FE simulation and generate the J-R curve.

4.6 Conclusions:

1. The Gurson parameters are not fully independent of each other and as a result, it is possible to obtain more than one set of parameters having similar effect on material behaviour.
2. The final slope of the engineering Stress-Strain curve is not much affected by the initial void volume fraction (f_o), though the point of failure is somewhat affected. This parameter may be used for finer tuning.
3. The final slope and failure point in Eng. Stress-Strain curve is affected almost most drastically by the critical void volume fraction (f_c). This parameter is used to calibrate the initial drop in slop.
4. The effect of the final void volume fraction (f_f) on Eng. Stress-Strain curve is nominal. While the slope is somewhat affected. This parameter helps in tuning of the final drop.
5. The value of nucleating void volume fraction affects the fracture strain. Lower values of fn yield stress-strain curve similar to elasto-plastic nature. This parameter helps is determining the total range of the curve after ultimate point.
6. By comparing the figs. (4.5 a to d) it is seen that every parameter starts its effect at some distinct point and modifies the curve further. This effect zone can be exploited during calibration.

7. Same Gurson parameters are used for both un-irradiated and irradiated specimen showing invariance of Gurson parameter for low dpa (i.e. 1.5 dpa). This is due to the fact that irradiation induces nano-voids which cause hardening by providing resistance to dislocation flow. So irradiation changes are reflected only on the stress strain data and not on Gurson parameters as they edict the mechanisms of micro void which causes softening in contrary to hardening caused by nano voids caused by irradiation .

Chapter 5

CLOSURES

5.1 Concluding Remarks

In the present work, aging study due to irradiation, which is the prime mode of degradation in nuclear reactor components, is studied with the aid both experimental and numerical. As remarked earlier that mainly experimental analysis of irradiated damage is cited in the previous literature. So a combined experimental and simulation approach is taken to deal with the problem at hand. Conclusions due to the present investigation is stated below

- ✓ For experimental study one of the most crucial parts is the fabrication of miniaturized specimen. Initial idea on dimension is derived from previous literatures. Also other constraints like damage depth in proton irradiation (depends on energy, as discussed in section 3.4.2), beam area and limit switch constrains by the DMA.
- ✓ After fabricating desired tensile specimen, testing of specimens of un-irradiated is done and repeatability of the results obtained is checked by finding out COV of the experiments.
- ✓ The obtained results are compared with standards (ASTM-370).It is observed that the ultimate strength obtained from miniaturized specimen is applicably less. This is due to the fact that only few grains are present in the thickness direction of the specimen and hence less hindrance to dislocation is encountered.
- ✓ The desired specimen is then sent to VECC for irradiation (by 9.5 MeV proton beam) to dpa levels of 0.01, 0.02, 0.04 and 0.06. (details of experimentation in table 3.6-3.9) The obtained dpa level is cross checked with the help of the count (which shows the total amount of current passing through the beam area) and software SRIM. SRIM calculations helps to determine the no. of vacancies per ion generated and with the help of eq.(3.2) dpa is calculated.
- ✓ After irradiation the samples are activated since the column barrier is about 7 MeV whereas the energy of the protons used is about 9.5 MeV. So the irradiated samples are in cooling time and once the activity will be under desired level testing will be proceeded.

- ✓ Due to unavailability of irradiated stress-strain data for irradiated materials from the above mentioned experiments, irradiated specimen data is obtained from literature [17]. Using these stress- strain data an advanced elasto-plastic simulation is carried out using G-T-N parameterized model.
- ✓ As G-T-N is a parameterized model, parametric study is conducted on parameters which are material variant (f_i, f_n, f_c and f_f). The other parameters are assigned default values found in the literatures.
- ✓ Parameter studies indicate that the effect of f_i on the stress strain curve is quite negligible and only affects the failure strain of the material (fig.4.5 a). Parameter f_c affects the stress-strain curve quite drastically as it signifies the void fraction at which coalescence through local instability occur (fig.4.5 b). The parameter fn signifies the volume fraction of no. of site at which nucleation can occur (fig. 4.5 c). Parameter f_f signifies the volume fraction of voids at which complete loss of strength takes place (fig 4.5 d).
- ✓ From the parametric studies stated above, calibration of gurson parameters is done for all dose levels (i.e. 0, 0.06 0.6 and 1.5 dpa). It is found that the Gurson parameters remain invariant under irradiation. As irradiation causes hardening by introduction of nano-voids, gurson parameters dictate the mechanism of micro voids which causes softening. So during elasto-plastic analysis hardening is only reflected by change in the stress strain data and not the gurson parameters.
- ✓ Finding out the gurson parameters can be very useful as it helps the analysis of toughness. Section 4.5.3 talks about the methodology by which a growing crack analysis can be done.

5.2 Significant Contribution of the Thesis

The contributions of the present research work are as follows:

- ➢ Fabrication of miniaturized specimen has been done satisfying the condition of available irradiation facility and testing machine. Also proton beam energy consideration has been accounted for.

- Irradiation via proton has been carried out at different dpa levels for the miniaturized specimens
- Un-irradiated material testing and comparison with standard results was done.
- Advanced elasto-plastic simulation using parameterized G-T-N model was employed to study both un-irradiated and irradiated material response. From this work it was concluded that the Gurson parameters remained invariant under irradiation.
- Methodology for growing crack analysis using the above mentioned calibrated gurson model is proposed.

5.3 Future Scope of the Research

- Due to miniaturization of testing specimen, size effect due to grain orientation and critical thickness (ratio of thickness to grain size) come into picture. These size effects can be incorporated by using Crystal plasticity studies.
- In this present work only irradiation damage is considered. But more complex degradation occurs due to the synergic effect of temperature creep and irradiation. Hence ore mathematically complex models can be made to incorporate these other modes of damage.
- Irradiation studies for higher dpa can be conducted.

References

1. Olander D.R., Radiation Damage. Ref. Ch.17 Fundamental Aspects of Nuclear Reactor Elements (1975).
2. Klueh R.L., Miniature Tensile Test Specimen for Fusion Reactor Irradiation Studies. Nuclear Engineering and Design/Fusion 2 (1985) 407-416.
3. Panayotu N.F., Puigh R.J., and Opperman E.K., Miniature Specimen Tensile Data for High Energy Neutron Source Experiments. Journal of Nuclear Materials 103 & 104 (1981) 1523-1526.
4. Chen C.Q., Sun J.G., and Xu Y.C., Neutron irradiation hardening of ODS alloy tested by miniature disk bend test method. Journal of Nuclear Materials 283-287 (2000) 1011-1013.
5. Dai Y., Long B., and Tong Z.F., Tensile properties of ferritic/martensitic steels irradiated in STIP-I. Journal of Nuclear Materiasl 377 (2008) 115-121.
6. Rabenberg E.M., Jaques B.J., Sencer B.H., Garner F.A., Freyer P.D., Okita T., and Butt D.P., Mechanical behavior of AISI 304SS determined by miniature test methods after neutron irradiation to 28 dpa. Journal of Nuclear Materials 448 (2014) 315-324.
7. Porollo S.I., Dvoriashin A.M., Vorobyev A.N., and Konobeev Yu. V., The microstructure and tensile properties of Fe-Cr alloy after neutron irradiation at 4000C to 5.5-7.1 dpa. Journal of Nuclear Materials 256 (1998) 247-253.
8. Olbricht J., Bismark M., and Skrotzki B., Characterization of creep properties of heat resistant 9-12% Cr steel by miniature specimen testing. Material Science and Engineering A 585 (2013) 335-342.
9. Pahlavanyali S., Rayment B., Roebuck B., Drew G., Rae C.M.F., Thermo-mechanical fatigue testing of superalloys using miniature specimen. International Journal of Fatigue 30 (2008) 397-403.
10. Kartal M., Molak R. Turski M., Gungor S., Fitzpatric M.E., and Edwards L., Determination of Weld metal mechanical properties utilizing novel tensile testing methods. Applied Mechanics and Materials Vol.7-8 (2007) pp 127-132.
11. Molak R.M., Kartal M., Pakiela Z., Manaj W., Turski M., Hiller S., Gungor S., Edwards L., and Kurzydlowski K.J., Use of Micro Tensile Test Samples in Determining the

Remnant life Pressure Vessel Steels. Applied Mechanics and Materials Vol 7-8 (2007) pp 187-194.

12. Sharpe W. N. ,Jr, Danley D., LaVan D.A, Micro-specimen Tensile Test of A533-B Steel, Small Specimen Test Technique, ASTM STP 1329 (1998) pp 497-512.
13. Marini B., Carassou S. ,Wident P. and Soulat P., Evaluation of the Fracture Toughness of a C-MN steel using Small Notched Tensile Specimen. Small Specimen Test Technique, ASTM STP 1329 (1998) pp 513-522.
14. Igata N., Miyahara K., Uda T., and Asada S., Effect of Specimen Thickness and Grain Size on the Mechanical Properties of Type 304 and 316 Austenitic Stainless Steel. The Use of Small-Scale Specimen for Testing Irradiated Material, ASTM STP 888 (1986) pp 161-170.
15. Rickerby D.G., Fenici, P., Jung, P., Piatti, G., and Schiller, P., Comparison of Mechanical Properties in Thin Specimens of Stainless Steel with Bulk Material Behavior. The Use of Small-Scale Specimen for Testing Irradiated Material, ASTM STP 888 (1986) pp 220-232.
16. Byun T.S., Kim J.H., Chi, S.H., and Hong, J. H., Effect of Specimen Thickness on The Tensile Deformation Properties of SA508 C1.3 Reactor Pressure Vessel Steel. Small Specimen Test Techniques, ASTM STP 1329 (1998) pp 575-587.

17. Matijasevic M., Almazouzi A., Effect of Cr on the mechanical properties and microstructure of Fe-Cr model alloy after n-irradiation. Journal of Nuclear Materials 377 (2008) 147-154
18. Needleman A., Tevergaard V., and Hutchinson J.W., Void Growth in Plastic Solids;
19. Cricri G., Consistent use of Gurson-Tevergaard damage model for R-curve calculation. Convegno Nazionale IGFXX, Torino 24-26 giugno (2009), 138-150.
20. Zheng C., Cesar de sa J.M.A., and Andrade Pires F.M., A Comparison of models for ductile fracture prediction in forging. Computational Methods in Material Science (2007) Vol.7, No. 4.
21. Pardoen T., and Hutchinson J.W., An extended model of void growth and coalescence. Journal of Mechanics and Physics of Solids 48 (2000) 2467-2512.

22. Feucht M., Dong-Zhi Sun, Erhart T., and Frank T., Recent devolopment and application of the Gurson model. 5. LS-DYNA Anwenderforum,Ulm (2006).
23. Hao S., Liu W.K., and Chang C.T.,Computer implementation of damage models by finite element and mesh free method. Comput. Methods Appl. Mech. Engrg. 187(2000) pp 401-440.
24. Tvergaard V., Hutchinson J.W., Two mechanism of ductile fracture: void by void growth versus multiple void interaction. International Journal of Solid and Structures 39 (2002) 3581-3597
25. Li Y.N., Karr D.G., and Wang G., Mesh Size Effect in Simulating Ductile Fracture of Metals. ABS TECHNICAL PAPERRS (2007)
26. Benzerga A.A., and Leblond J.B., Ductile Fracture by Void Growth to Coalescence. To appear in Advances in Applied Mechanics.
27. Was G. S, Fundamentals of Radiation Material Science, New York, Springer, 2007.

Appendix

This section contains some of the basic MATLAB coding used in the above work

1. Strain Rate computation:-

```
clear
clc
d=input('Enter displacement set=');
t=input('Enter time set=');
deld=diff(d);
delt=diff(t);
rt=zeros(length(delt),1);
for i=1:length(delt)
    rt(i)=deld(i)/delt(i);
end
mnrt=mean(rt);
mxrt=max(rt);
minrt=min(rt);
```

2. Nonlinear Fitting

```
function [fitresult, gof] = createFit1(tpstrain1, tstress1)
%CREATEFIT1(TPSTRAIN1,TSTRESS1)
%  Create a fit.
%
%  Data for 'untitled fit 1' fit:
%      X Input : tpstrain1
%      Y Output: tstress1
%  Output:
%      fitresult : a fit object representing the fit.
%      gof : structure with goodness-of fit info.
%
%  See also FIT, CFIT, SFIT.
%  Auto-generated by MATLAB on 07-May-2015 12:03:37


%% Fit: 'untitled fit 1'.
[xData, yData] = prepareCurveData( tpstrain1, tstress1 );

% Set up fittype and options.
ft = fittype( '244.19+a*x^b', 'independent', 'x', 'dependent', 'y' );
opts = fitoptions( ft );
opts.Display = 'Off';
opts.Lower = [-Inf -Inf];
opts.StartPoint = [0.438744359656398 0.381558457093008];
opts.Upper = [Inf Inf];
% Fit model to data.
```

```
[fitresult, gof] = fit( xData, yData, ft, opts );
% Create a figure for the plots.
figure( 'Name', 'untitled fit 1' );

% Plot fit with data.
subplot( 2, 1, 1 );
h = plot( fitresult, xData, yData );
legend( h, 'tstress1 vs. tpstrain1', 'R0073', 'Location', 'NorthEast' );
% Label axes
xlabel( 'tpstrain1' );
ylabel( 'tstress1' );
grid on
% Plot residuals.
subplot( 2, 1, 2 );
h = plot( fitresult, xData, yData, 'residuals' );
legend( h, 'R0073- residuals', 'Zero Line', 'Location', 'NorthEast' );
% Label axes
xlabel( 'tpstrain1' );
ylabel( 'tstress1' );
grid on
```

3. Hardening data generation

```
%Experimental analysis
clear
clc
SSc=input('Enter the Stress-Strain data=');
a=input('Enter the index of yeild point=');
b=input('Enter the index of ultimate point=');
c=input('If strain value is in % enter 1 else 0=');
%Loop to extract engg. stress strain data
if c==0;
 estrain1=SSc(a:b,1);
 estress1=SSc(a:b,2);
end
if c==1;
 estrain1=(SSc(a:b,1))/100;
 estress1=SSc(a:b,2);
end
plot(estrain1,estress1)
  hold on
d=input('Yield point problem. enter 1 for yes 0 for no=');
if d==0
   E1=estress1(1)/estrain1(1);
end
if d==1
   e=input('Avg Yield point=');
   if c==0
       E1=(SSc(e,2))/(SSc(e,1));
   end
   if c==1
       E1=(SSc(e,2))/((SSc(e,1))/100);
   end
end
    tstress=(estress1).*(1+estrain1);
    tstrain=log(1.+estrain1);
```

```
tpstrain=tstrain-(tstress./E1);
tpstrain1=tpstrain(5:length(tpstrain));
tstress1=tstress(5:length(tstress));
```

4. Gurson Surface generation

```
[Y,X,Z] =ndgrid(linspace(0,50,45),linspace(0,50,45),linspace(0,50,45));
% V = Y.^2+Y.^2-(sin(Z)).^2; % evaluate your implicit function
SGy=input('Enter the value of Yeild Stress=');
SGeq=sqrt(((((X-Y).^2)+((Y-Z).^2)+((Z-X).^2))/2));
SGm=(X+Y+Z)/3;
f=input('Enter the value of void volume fraction=');
q1=1.5;
q2=1;
q3=q1^2;
Phi=(((SGeq).^2)/(SGy^2))+(2*q1*f*cosh(1.5*q2*(SGm/SGy)))-(1+q3*(f^2));
% % p = patch(isosurface(X,Y,Z,Phi,0));
% % isonormals(X,Y,Z,Phi,p);
% set(p,'FaceColor','b','EdgeColor','k','FaceAlpha',0.5);
Shi=((SGeq.^2)/(SGy^2))-1;
% over the N-D grid
q = patch(isosurface(X,Y,Z,Shi,0));
hold on
isonormals(X,Y,Z,Shi,q);
set(q,'FaceColor','r','EdgeColor','k','FaceAlpha',0.5)% ou
% 'EdgeColor','none'
daspect([1 1 1])
%  axis square;
grid on;
% camlight
%  view(45,45);
% lighting gouraud
```